CIVIL ENGINEERING STUDIES

STRUCTURAL RESEARCH SERIES NO. 56

THE FATIGUE PROPERTIES OF WELD METAL

By
R. B. MATTHIESEN
and
L. A. HARRIS

Approved by
N. M. NEWMARK

UNIVERSITY OF ILLINOIS
URBANA, ILLINOIS

THE FATIGUE PROPERTIES OF WELD METAL

By

R. B. Matthiesen

and

L. A. Harris

Approved by

N. M. Newmark

A Report of an Investigation Conducted by

THE DEPARTMENT OF CIVIL ENGINEERING

UNIVERSITY OF ILLINOIS

In Cooperation with

THE OHIO RIVER DIVISION LABORATORIES

CORPS OF ENGINEERS

U. S. ARMY

Contract No. DA-33-017-eng-180

UNIVERSITY OF ILLINOIS

URBANA, ILLINOIS

JUNE 30, 1953

ACKNOWLEDGMENT

This report is part of the final report of a cooperative research project conducted in the Engineering Experiment Station of the University of Illinois, Department of Civil Engineering, and sponsored by the Ohio River Division Laboratories, Corps of Engineers, U. S. Army, under Contract No. DA-33-017-eng-180.

The work constitutes a part of the structural research program of the Department of Civil Engineering under the general direction of N. M. Newmark, Research Professor of Structural Engineering, and W. H. Munse, Research Associate Professor of Civil Engineering. The research was performed by L. A. Harris, Research Associate in Civil Engineering, who was the immediate Project Supervisor, and R. B. Matthiesen, Research Assistant in Civil Engineering.

The Authors acknowledge the assistance of the members of the fatigue Committee of the Welding Research Council, who acted in an advisory capacity.

The metallurgical studies were performed in the laboratories of the Department of Mining and Metallurgical Engineering, University of Illinois, under the supervision of R. W. Bohl, Assistant Professor of Metallurgical Engineering.

CONTENTS

Page No.

FIGURES

FIGURES (cont.)

TABLES

THE FATIGUE PROPERTIES OF WELD METAL

I. INTRODUCTION

1. Object of Investigation

One of the important recent contributions related to the science of welding has been the discovery and subsequent investigation of the effects of hydrogen in steel. In the welding of the more hardenable steels, the damage caused by hydrogen may be quite extensive, causing a reduction in the strength and ductility of the joint as a whole. The hydrogen, introduced into the weld from the gaseous shield provided by the burning of the electrode coating, may cause cracking in the heat-affected zone or micro-cracking in the weld metal, and may contribute to the porosity of the weld metal. In the welding of plain carbon structural steels, the effects of hydrogen are generally less severe than for the higher carbon steels. The weld may be subject to embrittlement of the weld metal, especially under conditions of rapid low temperature cooling rates.

The recent development of the low hydrogen type electrode has offered a solution to many of the problems associated with the presence of hydrogen in welds. However, even in solving these problems, the use of the low hydrogen electrode adds to the ever

present need for research by posing the question: What are its limitations?

The purpose of the present investigation is to determine and to compare, quantitatively, the fatigue and the static properties of weld metal deposited with the low hydrogen E7016 electrode and with the high cellulose E6010 electrode*.

During welding, the coating of the low hydrogen E7016 electrode, consisting largely of inorganic minerals, produces a gaseous envelope which has a low hydrogen content. Because moisture in the electrode coating can contribute to the hydrogen present in the arc atmosphere, special baking procedures are used with this electrode to reduce the moisture content of its coating. Protection of the weld is also provided by the formation of a thick friable slag which completely covers the weld metal.

In contrast, the coating on the commonly used high cellulose E6010 electrode contains a high percentage of organic materials, which decompose during welding to produce a protective gaseous atmosphere having a high hydrogen content. As additional protection to the weld metal, the coating produces a thin friable slag which generally does not completely cover the weld metal.

---

* The designations E6010 and E7016 are somewhat misleading, since the tensile tests of all-weld-metal specimens performed as a part of this investigation (see Section 16) indicate that the particular electrodes employed for these tests deposited weld metal having equal tensile strengths of about 70,000 psi.

Several previous investigations (1,2,3,4)* have compared the bend properties of bead-on-plate welds produced from low hydrogen E6016 and from high cellulose E6010 electrodes. For welds deposited from E6010 electrodes, the bend properties were each reduced by an increase in the severity of the low temperature cooling rate imposed on the weld. Micro-cracks were believed to have caused this embrittlement of the rapidly cooled "high hydrogen" weld metal. In contrast, none of the bend properties of welds deposited from E6016 electrodes were reduced, and the weld metal, even when subjected to the severest cooling condition employed, appeared to be free from micro-cracks. Further investigation of the micro-cracks showed that they were oriented transversely to the direction of welding.

On the basis of this information, the following hypotheses were formulated: (1) the fatigue strength of E7016 weld metal might be relatively high, since previous investigations have shown that weld metal deposited from this type of electrode generally has superior mechanical properties and is not subject to "hydrogen embrittlement"; (2) the fatigue properties of E6010 weld metal might be reduced by the presence of micro-cracks; and (3) because of the orientation of the micro-cracks, their greatest effect on the fatigue strength of the E6010 weld metal might occur when the weld is stressed in a direction parallel to the direction of welding.

---

* Numbers in parentheses refer to the list of references at the end of the paper.

2. Description of Tests

Four series of fatigue tests were performed. In Series A, the specimens were machined entirely from weld metal and were stressed longitudinally, parallel to the direction of welding. In both Series B and Series C, the specimens were stressed transversely to the direction of welding and contained weld metal, heat-affected zone, and base metal. Series B specimens had the weld metal centered in the test section with the fusion lines outside of the test section, whereas Series C specimens had the heat-affected zone centered in the test section. Series D specimens were machined entirely from the base metal.

In order that a correlation with full scale welded joints might exist, a fatigue specimen was desired in which a relatively large volume of weld metal would be subjected to a uniform stress. Therefore, specimens having a 3/8 in. diameter test section 1/4 in. long have been tested in axial tension with the stress cycle varying from a minimum tension of approximately 1000 psi to a maximum tension. A weldment was selected from which specimens could be prepared so as to stress the weld metal either (a) longitudinally, parallel to, or (b) transversely to the direction of welding. The weldments prepared from each of the two types of electrodes were subjected to one of the following conditions: (1) preheating, or (2) water quenching two minutes after welding. These conditions were selected to establish the range of variation in weld metal fatigue properties which might occur in service.

Three series of specimens were tested to determine the static tensile properties of welds prepared in the same manner as those which were employed in the fatigue investigation: (1) the type AT longitudinal weld specimen, which contained only weld metal; (2) the type BT transverse weld specimen, which contained weld metal, heat-affected zone, and base metal; and (3) the type DT plain plate specimen, in which the base material was stressed transversely to the direction of rolling.

In addition to the fatigue and static tests, the following supplementary tests have been performed: chemical analyses of the base plate and of the weld metal deposited from the two types of electrodes, and hydrogen analyses and metallurgical investigations of both types of weld metal which had been subjected to each of the welding conditions.

II. PREPARATION AND EXAMINATION OF WELD SPECIMENS

3. Welding Procedures

As previously indicated, the low hydrogen E7016 and the high hydrogen E6010 electrodes were used in this investigation. Since moisture in the electrode coating can contribute materially to the hydrogen absorbed in the weld metal, the low hydrogen electrodes were oven dried at a temperature of approximately 220 deg. F. for a period of one week prior to use. A drying procedure is usually recommended for the low hydrogen electrode, but not for the high hydrogen E6010 electrode because a slight amount of moisture has a beneficial effect on the operating characteristics of this electrode. However, the drying procedure noted above was used with the high hydrogen electrodes to limit the hydrogen present in the weld atmosphere to that produced by the decomposition of the electrode coating. A limited study of the effect of different welding procedures (see Section II) indicated that the drying of the E6010 electrode did not have an adverse effect on its fatigue properties.

The weld specimens were prepared from a semi-killed steel which was ordered to ASTM designation A7. The physical properties and the chemical analysis for this plate are presented in Tables 1 and 2, respectively. This steel is from the same heat as that designated as Steel "B" in a previous investigation, "Effects of Hydrogen and Related Variables on the Physical Properties of Welds

on Structural Steels" (4). The location of the required material in the parent plate is shown in Fig. 1.

Multiple pass welds were manually deposited in a single V joint having a 45 degree included angle and a 1/2 in. root spacing. The joint was formed by 3/4 in. plates and a 1/4 in. back-up strip. Generally, the weldments were 12 1/2 in. wide and 4 1/2 in. long. However, some weldments were made 6 in. long so that one chemical analysis sample and one longitudinal tensile coupon could be prepared from the same weldment. The details of both types of weldment are shown in Fig. 2. The welding procedure employed eleven passes, each pass being deposited with a single electrode and with alternate passes being welded in opposite directions to heat the weldment uniformly along its length.

The welding power was supplied by a 400 ampere capacity direct current generator of standard manufacture. To secure duplication of welding conditions from one specimen to another, the generator was adjusted to give the desired current and voltage indications on portable meters which were connected as close to the arc as practical. The welding variables used for the two electrode types are as follows:

Electrode	Size	Current	Voltage	Open Circuit Voltage	Average Rate of Travel	Burn-off Rate
	in.	amps.	volts	volts	in./min.	in./min.
E6010	3/16	170	24	84	4.2	9.5
E7016	3/16	200	20	84	4.2	9.3

In order to establish the range of variation in fatigue properties which might occur in service, the welds were either preheated or water quenched two minutes after welding. These conditions were selected on the basis of a previous investigation (4) in which a study was made of the static bend properties of bead-on-plate welds. For the preheated specimens, the weldments were furnace preheated to 450 deg. F. for one hour, and were allowed to air-cool for five minutes between passes. It was determined by measurements with a contact pyrometer that air-cooling for five minutes allowed the weld metal to cool to a temperature of between 450-500 deg. F. Thus, all passes were deposited with the temperature of the weldment at the preheat temperature.

In contrast, the quenched specimens were not preheated and were cooled between passes by being water quenched two minutes after welding. The water bath was maintained at a temperature of about 56 deg. F. by a continuous flow of water. After quenching, the weldment was dried in a stream of air before deposition of the succeeding pass. The temperature of the weld metal was found to be 300-350 deg. F. at the time of quenching.

In comparing the results from the tests of preheated and of quenched welds, the effects of the difference in the heating and cooling cycle must be considered. This difference in the heating and cooling cycle is evidenced by a comparison of the temperature of the preheated specimens 5 minutes after welding (450-500 deg. F.) with the temperature of the quenched specimens 2 minutes after welding (300-

350 deg. F.). Thus, the weld metal of the preheated specimens is subjected to a more thorough heat treatment by the deposition of succeeding passes than is the weld metal of the quenched specimens.

4. Chemical Compositions of Weld Pads

A comparison was made between the chemical compositions of the weld metal deposited from each type of electrode. Also, because more than one container of electrodes of each classification was used, it was desired to determine whether the electrodes from the different containers deposited weld metal having the same chemical composition and physical properties. For this purpose, the 6 in. long weldments were used to prepare both a tensile coupon and a chemical analysis sample.

A study of the tensile properties, discussed in Section 16, indicated that the weld metal deposited by electrodes of the same classification but from different containers had the same strength and ductility.

The chemical analysis samples were prepared from the material along the centerline of the weld through its thickness, and the results of the analyses are summarized in Table 3. The variation of chemical composition is as could be expected for weld metal samples. Comparison of the two types of weld metal indicates that for the E6010 weld metal, the carbon content is slightly lower, the manganese content is higher, and the silicon content is lower than for the E7016 weld metal.

5. Hydrogen Contents of Weld Pads

Analyses were performed on all-weld-metal samples to determine the hydrogen contents of the E7016 and the E6010 weld metals subjected to the preheated or the quenched conditions. Three adjacent 1/4 in. cubes were cut from the center of each type of weld metal. The material was taken from a transverse 1 in. slice similar to those used to prepare the transverse fatigue specimens. The specimens were welded in the morning, cut on a metallurgical cut-off-wheel, filed, cleaned in CP acetone and benzene, and stored over night in a refrigerated box at a temperature of -60 deg. F. At 8 o'clock the following morning, they were removed from refrigeration and analyzed during the same day at a commercial laboratory* using an analysis train similar to that reported by Carney, Grant, and Chipman (5), modified to analyze for hydrogen by a calibrated thermal conductivity cell.

The results of the analyses, presented in Table 4, indicate that there was a large amount of hydrogen (about 10 parts per million) present in either the preheated or the quenched E6010 weld metal; whereas relatively little hydrogen (about 1 part per million) was present in the E7016 weld metal. It is important to note that hydrogen was present in the weld metal deposited with the low hydrogen electrode. The amount of hydrogen observed is in substantial agreement with the amounts reported by several other investigators. Any differences which

---

* Anderson Physical Laboratory, Champaign, Illinois

might exist between the hydrogen contents of the preheated or the quenched weld metals could not be determined because of the limited number of tests.

In a subsequent investigation of double-V butt welded joints prepared with the same electrodes, the hydrogen content of the E6010 weld metal was found to be about 3.0 parts per million. Thus, in comparison, tests of all-weld-metal specimens are more apt to be influenced by the effects of hydrogen than are tests of double-V butt welds.

6. Macro-Examinations of Weld Cross-Sections

In order to observe differences in the structure of the weld metal subjected to the preheating or to the quenching procedures, macro-examinations of a transverse section of the weld pads were made. The specimens were first ground on a belt grinder, then mechanically polished on emery paper through successive stages as follows: No. 1, No. 0, No. 2/0, and No. 3/0. Three stages of wet grinding beyond the emery were used: No. 600 alundum, No. 303½ emery, and 5 micron alumina. The specimens were etched with a 2 percent nital solution.

The macrographs of the preheated and of the quenched weldments prepared from both types of electrodes are presented in Fig. 3. A comparison of the quenched and the preheated specimens indicates two major differences in the appearance of the weld cross-sections. First, the heat-affected zone of the preheated specimens is significantly wider than that of the quenched specimens. Secondly,

most of the weld metal of the preheated specimens had been recrystalized by the heat treatment of succeeding passes, whereas a considerable proportion of the quenched weld metal had not been recrystallized. Such differences are to be expected as a consequence of the difference in the heating and cooling cycles of the preheated and the quenched specimens.

Further observation indicates that defects are present in both the preheated and the quenched E7016 sections and in the preheated E6010 section. The most prominent defects, those present in the preheated E6010 weld cross-section, were located in the weld metal and are probably gas pockets. Both specimens deposited by the E7016 electrode contained defects at the fusion line, which could be either inclusions, gas pockets, or regions of non-fusion with the base metal. No defects were visible in the quenched E6010 cross-section.

7. Hardness Surveys of Weld Cross-Sections

The specimens which were prepared for the macro-examination were subsequently used for the hardness surveys. The polished and etched surfaces were indented with a 136 degree Vickers diamond indenter on a Tukon Hardness Tester using a load of 1 kilogram.

For each specimen, hardness readings, spaced 2 mm apart, were taken along three horizontal and three vertical lines as shown at the top of Table 5. The middle line of the horizontal readings was positioned at the mid-depth of the plate and the other two lines were spaced approximately 6 mm on either side of this center line. For the vertical readings, the middle line of the readings coincided

with the vertical centerline of the weld metal, and the outer two lines passed through the center of the heat-affected zone at the mid-depth of the plate.

The results of the hardness surveys are summarized in Table 5, in which the average hardness and range is given for all of the readings in the weld metal, the heat-affected zone, and the base metal. For the weld metal, separate results for each of the three horizontal lines are also presented.

The quenching and the preheating procedures appear to affect the hardness of the E6010 and the E7016 weld metals differently. For the E6010 weld metal, the hardness increased from an average value of 153 for the preheated condition to 185 for the quenched condition. On the other hand, the average hardness of the E7016 weld metal remained practically constant, being 169 and 167 for the preheated and the quenched conditions, respectively. Thus, only the hardness of the E6010 weld metal appears to be greater for the quenched condition.

A comparison of the three horizontal lines of hardness readings in the weld metal indicates a difference between the preheated and the quenched specimens. In the preheated condition, the E7016 weld metal shows a consistent decrease in hardness from 178 at the top horizontal line to 153 at the bottom horizontal line. The preheated E6010 weld metal showed only a slight decrease in hardness from 153 at the top line to 148 at the bottom line. The decrease in hardness with depth correlates with the longer heat treatment of the first passes and the successively shorter heat treatments of the later passes.

The quenched specimens do not exhibit this trend of decreasing hardness through the thickness of the weld deposit.

There were not sufficient points taken in the heat-affected zone to draw any definite conclusions regarding this region. Both the E6010 and the E7016 weld specimens appear to reflect a higher hardness for the quenched condition, but it is not possible to determine whether any difference existed between the hardness of the heat-affected zones of the E6010 and the E7016 welds.

The hardness of the base plate averaged from 139 to 157, and that of the back-up strip from 116 to 126.

8. Micro-Crack Investigations of Weld Metal

As stated in the introduction, it has been found that micro-cracks are present in weld metal deposited by E6010 electrodes under conditions of rapid low temperature cooling rates. In order to determine whether micro-cracks occurred in the weld metal produced under the present test conditions, a crack survey was made on a vertical section along the center line of the weld metal. The specimens were processed by mechanical metallurgical polishing through successive stages of emery and were then wet polished, the final polish being made with a 5 micron alumina abrasive. The specimens were then given an electrolytic polish in a chrome acetic bath (135 ml acetic acid, 25 gm Cr_2O_3, and 7 ml of H_2O) for 2 to 3 minutes at 20 volts and a temperature of 15-19 deg. C.

After electropolishing, the specimens were mounted on a mechanical stage and observed at a magnification of 150X along three vertical traverses spaced at intervals of approximately 0.12 in. Each traverse covered a strip approximately 0.05 in. wide.

No cracks were observed for either the E6010 or the E7016 preheated specimens; however, cracks were observed in the weld metal of the quenched specimens from both electrodes. In specimen 62B47, a quenched E7016 specimen, 20 cracks were observed in the area surveyed; whereas in specimen 02B40, a quenched E6010 specimen, 108 cracks were observed in approximately the same area. The cracks were present at all depths of the specimen and were oriented approximately transversely to the direction of welding. Photomicrographs illustrating the size and shape of the cracks are shown in Fig. 4.

As noted above, micro-cracks are present in the quenched weld metal produced with either type of electrode. The relatively large number of micro-cracks in the weld metal deposited with the E6010 electrode is probably a function of the higher hydrogen content, but this cannot be proved by the data presented.

III. DISCUSSION OF FATIGUE TESTS

9. Machining Procedures

As previously indicated, the fatigue tests were conducted to determine the properties of weld metal stressed both longitudinally and transversely to the direction of welding. Therefore, "longitudinal" and "transverse" specimens were prepared from the weldments as indicated in Fig. 5. It is apparent from this figure that the longitudinal specimens contained only weld metal, whereas the transverse specimens contained weld metal, heat-affected zone, and base metal. For the transverse type B specimens, the weld metal was centered in the test section, with the heat-affected zones outside of the test section; for the transverse type C specimens, the center line of the specimen was located in the heat-affected zone 1/16 in. from the fusion line by polishing and etching the side of the specimen before it was machined. It should be noted that the base plate is stressed transversely to the direction of rolling in the transverse specimens.

Either one longitudinal specimen or four transverse specimens could be prepared from each weldment. Of the four transverse specimens prepared from any one weldment, no more than three were tested in fatigue so that the remaining specimens could be used for one of the tests reported in Chapters II or IV. Table 6 references the test specimens with their respective weldments and indicates the type of test for which each specimen was used.

To provide a basis for evaluating the fatigue strength of the transverse type C weld specimens, a series of specimens, type D, were prepared from the base plate material. These plain plate specimens were machined so that the applied stress would be transverse to the direction of rolling as in the type C specimens.

All of the fatigue specimens were machined in a lathe equipped with a hardened cam which guided the carriage so that the lathe tool would cut the desired contour. The finished specimens, shown in Fig. 6, were 4 in. long and had a test section 3/8 in. in diameter and 1/4 in. long. All of the fatigue specimens were polished in the direction of the applied stress with successively finer grades of aluminum oxide cloth and finished with a crocus cloth.

10. Testing Procedures

The fatigue tests were performed at room temperature in a 50,000 lb. capacity Wilson lever type fatigue machine which ran at a speed of approximately 300 cycles per minute. The essential features of the machine, shown in Fig. 7, are a variable throw eccentric which transmits force through a dynamometer (for determining the load on the specimen) to a lever which in turn transmits the force to the upper pull head at a multiplication ratio of approximately 10 to 1. The machine was adjusted to provide a stress cycle varying from a minimum tension of approximately 1000 psi to a maximum tension.

Since a uniform stress distribution was desired across the specimen, special precautions were taken to align the specimen in the

machine and to maintain this alignment throughout each test. First, pull heads with sperical seats (see Fig. 7) were added to the testing machine to reduce the eccentricity due to the initial seating of the specimen. The spheres were carefully lapped into their sockets to provide free movement of the parts when a specimen was placed in the machine. A mixture of powdered molybdenum disulfide and oil was used as a lubricant between the sphere and the socket. This combination was found to provide good lubrication while setting up the specimens and to prevent corrosion during the test. Secondly, side plates were added to keep the upper and the lower pull heads in line. These side plates were shimmed into position after the pull heads had been carefully alligned by applying a tensile load to the calibration weigh bar which was used to determine eccentricity. Finally, a pair of adjustable guide links were attached to the upper heads. These guide links controlled the direction of motion of the upper head and were adjusted to achieve a minimum bending of the specimen. Details of this apparatus are shown in Fig. 7.

In setting a specimen in the machine, the spheres and sockets were first thoroughly lubricated, and the specimen was screwed into the spheres and secured by lock nuts. Then, the spheres were rotated while subjected to a low stress to work them into place; the specimen was loaded to the desired stress; and the eccentric was adjusted to provide the desired range of stress.

To calibrate the fatigue machine, a 3/4 in. diameter calibrated weigh bar was put into the machine in place of the test specimen. The weigh bar had four strain gages spaced 90° apart around its

perimeter so that in addition to the total load on the specimen, the bending of the specimen could be readily determined. The weigh bar was calibrated in a 10,000 lb. capacity Olsen screw type testing machine.

The load applied to the specimens was determined from strain gages mounted on the dynamometer. This load measuring system was calibrated monthly and an average calibration constant of 19.80 pounds per micro-inch was used in computing the reported stresses. The maximum deviation in the calibration constant was 0.26 pounds per micro-inch, and the probable overall accuracy of the load determination was estimated to be 2 to 3 percent of the total load (or stress) applied to any specimen.

The variation in maximum bending stress on the 3/4 in. diameter weigh bar was determined from the data obtained during calibration of the machine. The bending stress can be easily converted into the eccentricity of loading. Typical plots of the bending stress and the eccentricity as functions of the average stress are shown in Fig. 8. It is apparent that the bending stress approaches a maximum value of about 1200 psi at a low value of average stress and then remains essentially constant. As a consequence, the eccentricity of loading is relatively high for small values of average stress, but reaches a value of about 0.005 in. for higher values of average stress.

Since polished, unnotched specimens were being tested, it was necessary to stress some specimens beyond their yield point. Therefore, in determining the load to apply to the specimen, the

"true" stress (based on the reduced area) was used. While the specimen was being loaded manually for the first cycle, the reduced area was determined by measuring the diameter with a 1/10000 in. cone-tipped micrometer, and the desired maximum load was determined so that the desired true stress was not exceeded.

The machine could be run continuously since it was equipped with a micro-switch which stopped the motor if the maximum deflection of the specimen increased. The load was checked frequently at the start of a test and then only as often as necessary to maintain the desired load.

Failure was generally reported as the number of cycles at which the machine was stopped automatically by the micro-switch as the result of the formation of a crack. However, for some specimens, failure is reported as the number of cycles at which a crack was first detected, even though the machine had not as yet stopped automatically. The maximum probable difference which might occur as a result of the different criteria of failure is estimated to be 10,000 cycles.

After a crack was formed, the specimens were pulled apart statically so that the fatigue fractures could be examined to determine the appearance and the point of initiation of failure. Therefore, the fracture surface of each specimen consisted of two fracture areas distinctly different in appearance: (1) an area of fatigue fracture, and (2) an area of static tensile fracture.

11. Results of Fatigue Tests of Longitudinal All-Weld-Metal Specimens - Series A

The specimens for Series A were prepared entirely from weld metal in such a manner that the stress was applied longitudinally to the direction of welding. As indicated in the preceding section, all of the fatigue tests performed as a part of this investigation were axial tension tests in which the stress on the specimen varied from a minimum of 1000 psi to a maximum value which is reported in the results.

In Table 7, the results for each specimen of Series A are summarized in terms of the yield point, the maximum nominal stress, the maximum true stress, and the number of cycles to failure. In addition, a brief description is given of the appearance of the fracture surface and the location of the point of initiation of the failure.

In considering the fatigue strength of the preheated E7016 weld metal, one should note that in order to cause failure, all of the specimens had to be stressed at or above their yield points. Particularly significant are the results from one of the preheated E7016 specimens, 60A14, which failed after 404,000 cycles at a nominal stress of 68,000 psi. This stress is approximately equal to the maximum nominal static strength of the preheated E7016 weld metal, as determined by the tensile tests reported in Chapter IV. Thus, polished specimens of preheated E7016 weld metal have a high resistence to repeated loads even at stresses approaching the maximum nominal static strength of the material.

Only two of the quenched E7016 weld metal specimens showed a definite yield point when being loaded manually for the first cycle; however, all of the specimens were tested at or above their yield points as determined by the tensile tests.

In contrast to the E7016 weld metal, which was subjected to stresses in the plastic range, only one specimen of the E6010 weld metal was tested at a stress above its yield point. This latter specimen failed after only 74,000 cycles at a nominal stress of 56,500 psi.

The SN diagrams (Stress as a function of Number of cycles to failure) for the type A specimens have been plotted in terms of true stress in Fig. 9 and in terms of nominal stress in Fig. 10. Note that only those specimens which are tested at stresses above their yield points will have different true and nominal stresses. The effect of plastic straining must be kept in mind when comparing the results from the tests of the E7016 and the E6010 weld metals.

It is apparent from an examination of the SN diagrams that the fatigue strength of the E7016 weld metal, especially that of the preheated E7016 weld metal, is significantly greater than the fatigue strength of the E6010 weld metal. In terms of the nominal stress, the fatigue strength at a given number of cycles for the preheated E7016 weld metal is approximately 25,000 psi (nominal stress) greater than the fatigue strength of the preheated or the quenched E6010 weld metal. Similarly, the fatigue strength of the quenched E7016 weld metal is approximately 18,000 psi (nominal stress) greater than the corresponding fatigue strength of the E6010 weld metal either quenched or preheated.

The results also show that the E7016 weld metal quenched two minutes after welding has a fatigue strength about 7,000 psi (nominal stress) less than the fatigue strength of the preheated E7016 weld metal, but that the quenched and the preheated E6010 weld metals have approximately the same fatigue strengths. Any effect of quenching the E6010 weld metal appears to be masked by the effects of porosity or other defects.

Considerable experimental scatter is evident in the test results for each group of specimens, with the exception of the preheated E7016 weld metal. This scatter is probably related to the size, shape, distribution, and number of defects present in any particular specimen, although no direct correlation could be made on the basis of the appearance of the fractures. The scatter was especially pronounced for the preheated E6010 weld metal.

The fatigue strengths corresponding to failure at 100,000 and 2,000,000 cycles can be approximated from the SN diagrams and these values are summarized in the following chart.

Electrode	Condition	Fatigue Strength $f_{100,000}$		Fatigue Strength $f_{2,000,000}$	
		true psi	nominal psi	true psi	nominal psi
E6010	preheated	53,000	53,000	40,000	40,000
E6010	quenched	53,000	53,000	40,000	40,000
E7016	preheated	-	-	70,000	65,000
E7016	quenched	69,000	66,000	59,000	58,000

It was impossible to determine a fatigue strength for failure at 100,000 cycles for the preheated E7016 weld metal because the load could not be maintained above a nominal stress of approximately 68,000 psi (75,000 psi, true stress), which approaches the maximum nominal strength of this material.

As mentioned previously, after a fatigue crack had been formed and the test machine was stopped, the specimens were broken statically so that the fracture surfaces could be examined. Therefore, the fracture surface of each specimen consisted of two distinctly different fracture areas: (1) a flat, smooth, silky area of fatigue fracture, and (2) a coarser and sometimes rough appearing area which was fractured statically. A brief description of the appearance of each fracture is given in Table 7, and photographs of fracture surfaces for each of the four conditions (two conditions of welding and two electrodes) are shown in Fig. 11.

The most important conclusion drawn from the observations of the fractured specimens is that failure of all of the specimens produced from the E6010 electrodes originated at gas pockets. Some of these specimens failed at gas pockets on their surface, others failed at internal voids, and some failed at two or more gas pockets lying in different planes transverse to the direction of loading. The longest dimension of the gas pockets, as measured on the photographs of the fractured surfaces, was estimated to be between 0.03 and 0.10 in.

The fatigue fracture area of the specimens of preheated E6010 weld metal was usually a flat smooth circle concentric with the

gas pocket from which the fracture initiated. The tensile fracture area had a rough appearance, and all of the specimens contained gas pockets or other defects in this area.

Some of the quenched E6010 specimens had a fatigue fracture area which had much the same appearance as that of the preheated E6010 specimens; others had a somewhat rougher appearance. The tensile fracture area for all of the quenched E6010 specimens contained a large number of bright appearing areas in a rough fracture surface. Under microscopic examination, the small defects appeared to be cup-like surfaces oriented transversely to the axis of the specimens.

Only one of the specimens of preheated E7016 weld metal (60A10) had a visible defect thought to be the point of initiation of fracture (see Fig. 11b), and this defect, when examined under a microscope, appeared to be a crack oriented parallel to the axis of the specimen. Generally, the fatigue fracture of the preheated E7016 weld metal started at the surface of the specimen and was flat, smooth, and perpendicular to the direction of the applied stress. The tensile fracture had a ductile, shear-type appearance.

With one exception, the specimens of quenched E7016 weld metal failed at internal defects appearing to be gas pockets. However, the defects were small in comparison to the gas pockets in the E6010 weld metal. The tensile fracture area contained small bright defects in an otherwise ductile area, but the defects were neither as numerous nor as large as those in the quenched E6010 weld metal.

As previously mentioned, the specimens for Series A, B, and C were prepared using dried electrodes. When it was observed that porosity governed the fatigue strength of the E6010 weld metal, a limited study of preheated E6010 specimens was made to determine the effect of using the electrodes as-stored or artificially moistened, and of using an open-circuit voltage of 66 volts rather than the 84 volts which was used in the preparation of specimens for the main series of tests. The open-circuit voltage of 66 volts was selected after observing the operating characteristics of the electrode for various open-circuit voltages between 60 and 85 volts. The results of this investigation are summarized in Table 8 and are presented in an SN diagram in Fig. 12, wherein the results of the preheated E6010 specimens of type A are presented for comparison.

An improvement was noted in the operating characteristics of the as-stored and the moistened electrodes in comparison to the dried electrodes. However, all of the specimens prepared from the E6010 electrodes contained gas pockets regardless of the conditions employed in producing the weld; furthermore, the results of the fatigue tests indicate that drying did not have an adverse effect on the fatigue strength of the weld metal. Any improvement in the operating characteristics due to moisture in the electrode coating is not reflected in an improvement of the fatigue strength of the resultant weld metal. The effect of the lower open-circuit voltage on the fatigue strength may have been slightly beneficial.

12. Results of Fatigue Tests of Transverse Specimens with the Weld Metal Centered in the Test Section - Series B

This series of tests was intended to study the fatigue properties of weld metal stressed in a direction transverse to the direction of welding. The specimens were prepared with the weld metal centered in the test section and with the fusion lines situated outside of the test section.

The results, as given in Table 9 and Fig. 13, are erratic for all types of specimens. The fatigue strength of the transverse E6010 specimens appears to be about the same as the fatigue strength of the longitudinal E6010 weld metal (Series A), and all of the failures occurred at gas pockets either in the test section or near the fusion line. Photographs of the fracture surfaces of the type B specimens are shown in Fig. 14.

The fatigue strength of the transverse E7016 specimens appears to be lower than the fatigue strength of the longitudinal E7016 specimens, but all of the specimens failed outside of the test section. The failures of the preheated E7016 specimens appeared to be at the fusion line, whereas the failures of the quenched E7016 specimens occurred at defects in the weld metal at or near the fusion line.

Since failures occurred out of the test section at or near the fusion line, this series of tests was discontinued in favor of Series C in which the heat-affected zone is centered in the test section.

13. Results of Fatigue Tests of Transverse Specimens with the Heat-Affected Zone centered in the Test Section - Series C

For the type C specimen, the center of the specimen was located in the heat-affected zone 1/16 in. from the fusion line; therefore, the test section contains weld metal, heat-affected zone, and base plate. In Table 10, the results are summarized in terms of the yield point, the maximum nominal stress, the maximum true stress, and the number of cycles to failure. In addition, the appearance of the fracture surface and the point of initiation of fracture are reported where possible.

In the entire series, all but four of the specimens were tested at stresses above their yield points. The yield points observed while loading the specimen manually for the first cycle were all above the yield point of the base metal and below the yield point of the weld metal, as determined by the tensile tests reported in Chapter IV.

The SN diagrams for the type C series are presented in terms of true stress and in terms of nominal stress in Figures 15 and 16, respectively. The most notable feature of the test results is the large amount of scatter. The scatter is so great that little difference can be detected between the results from specimens prepared by different welding procedures, except for the quenched E7016 specimens which have a slightly higher resistance to fatigue. In terms of the nominal stress, the slope of the SN diagram is somewhat less than in terms of the true stress; however, the same amount of scatter continues to exist.

Because of the amount of scatter, the results, summarized in the following Table, are reported as a range of stress.

Electrode	Condition	Fatigue Strength $f_{100,000}$		$f_{2,000,000}$	
		true ksi	nominal ksi	true ksi	nominal ksi
E6010	preheated	42-53	42-51	37-47	37-47
E6010	quenched	45-56	44-56	39-50	40-52
E7016	preheated	48-54	48-52	43-48	43-47
E7016	quenched	-	-	49-53	51-53

No values for $f_{100,000}$ are reported for the E7016 preheated weld specimen because the load could not be maintained above a nominal stress of about 55,000 psi, at which stress failure generally occurred after about 400,000 cycles.

An examination of the fracture surfaces of the type C specimens, briefly described in Table 10, disclosed that all of the failures of the E6010 specimens originated at gas pockets in the weld metal or at defects at or near the fusion line. Some of the failures of the E7016 weld specimens originated at defects at or near the fusion line, whereas other failures originated at the surface of the specimen in base metal. Photographs of fracture surfaces are shown in Fig. 17. The appearance of the fracture surface in the weld metal depended on the welding procedure, but the fracture surface in the base metal was characterized by light striations in the fatigue fracture and by heavy striations in the tensile fracture.

All of the fatigue fractures of the preheated E6010 weld specimens initiated at gas pockets, remained entirely in the weld metal, and were flat, smooth, and shiny. Usually the tensile fracture was in the weld metal and had a ductile appearance, although for two specimens the tensile failure progressed into the base metal and had a rougher striated appearance in that region.

For the quenched E6010 specimens, one failure started from a defect at the fusion line, whereas the other failures started at gas pockets in the weld metal. Two specimens failed entirely in the weld metal, and were characterized by flat smooth fatigue fractures and rough tensile fractures containing numerous small bright surfaces. Although smaller and elongated in the transverse specimens, these bright surfaces are believed to be the same type of defect as the small bright cup-like surfaces observed in the quenched E6010 longitudinal type A specimens. For the remaining quenched E6010 specimens, the fatigue and tensile fracture areas were in both the weld metal, which contained gas pockets and small bright surfaces, and in the base metal, which was striated.

In four of the preheated E7016 specimens, failure originated at a defect (either an inclusion, a gas pocket, or a region of non-fusion) near or at the fusion line. Because of these defects, the fatigue fractures were rough and usually not flat. In the tensile fracture area, striations, characteristic of failure through the base metal, were evident in all of the specimens; although some specimens also contained small regions of weld metal in the tensile fracture area.

For the quenched E7016 specimens, the fatigue fractures initiated either at a defect in the weld metal or at the surface of the specimen. All of the specimens for which failure started at the surface appeared to have failed entirely in the base metal. For the specimen which failed at a defect, both the fatigue fracture and the tensile fracture were rough and appeared to be partially in the weld metal and partially in the base metal.

14. Results of Fatigue Tests of Plain Plate Specimens - Series D

To establish a basis of comparison for the type C fatigue specimens, a series of plain plate specimens, type D, were prepared so that the base metal would be stressed transversely to the direction of rolling.

The test results, summarized in Table 11, show that all of the specimens were stressed above their yield points. When plotted as an SN diagram (Fig. 18), the results appear to be consistent and indicate a fatigue strength of about 43,000 psi nominal stress (44,000 psi true stress) at 2,000,000 cycles. No value for the fatigue strength at 100,000 cycles could be determined because the load on the specimen could not be maintained at a stress above 46,000 psi nominal stress (50,000 psi true stress). This value is below the maximum nominal strength of the base material as determined by the tensile tests (Section 18), but is well within the range in which plastic flow takes place.

A comparison of the fatigue strengths of the base material and the type C weld specimens indicates that the quenched E7016 weld specimen had a higher fatigue strength (51,000-53,000 psi nominal stress at 2,000,000 cycles) than the plain plate specimen (43,000 psi nominal stress at 2,000,000 cycles), whereas the range of fatigue strengths reported for the preheated E7016 and for the preheated or the quenched E6010 weld specimens brackets the fatigue strength of the plain plate specimens.

As noted in Table 11, the fractures initiated at the surface for all of the plain plate specimens. The fatigue fracture area was flat and perpendicular to the direction of the applied stress, but was rough and contained light striations. In the tensile fracture area the surface was rough, jagged, and deeply striated. Photographs of the fractured surfaces are shown in Fig. 19.

IV. DISCUSSION OF STATIC TENSILE TESTS

15. Preparation of Tensile Specimens

The joint preparation and welding procedures used for the tensile specimens were the same as those used in the preparation of the fatigue specimens. Each type of electrode was used to prepare weld specimens which were subjected to one of the two conditions: preheating or water quenching two minutes after welding.

As indicated in Fig. 20, the tensile specimens had a test section with a 1/2 in. diameter and a 2 in. gage length. Successively finer grades of aluminum oxide cloth were used to polish the specimens in a direction transverse to the direction of the applied load. A 120 grit aluminum oxide cloth and oil were employed in the final polishing.

The type AT tensile specimen, which corresponds to the type A fatigue specimen, was machined entirely from weld metal and was stressed in a direction parallel to the direction of welding. In order to determine the physical properties of a weld specimen stressed transversely to the direction of welding, the type BT tensile specimen was machined from a strip cut transversely to the direction of the weld and contained weld metal, heat-affected zone, and base metal in the test section, as did the transverse type C fatigue specimen. Plain plate specimens, type DT, were machined so that the applied stress would be perpendicular to the direction of rolling, as in the transverse weld specimen.

As mentioned in Section 4, an investigation was made to determine whether the electrodes from different containers produced weld metal having the same tensile properties. Accordingly, four E6010 and four E7016 weld specimens were prepared, each specimen being welded with electrodes from a different container. Except that the welds were 6 in. long rather than 4 1/2 in. long, the joint preparation and welding procedures were the same as those employed in the preparation of the preheated specimen. Therefore, the results are discussed with those of the corresponding preheated type AT tensile specimen.

The specimens were tested in a 120,000 lb. capacity Baldwin hydraulic testing machine at a strain rate of 0.02 in. per min. During the test, diameter measurements were taken with a 1/1000 in. micrometer until the load fell off and necking became apparent. From the data taken during the test, both the true stress-true strain relationship and the nominal stress-strain relationship could be determined.

16. Results of Tensile Tests of Longitudinal Type AT All-Weld-Metal Specimens

The results of the tensile tests of the longitudinal type AT all-weld-metal specimens are summarized in Table 12 in terms of the yield point, the maximum nominal stress, the percent elongation, and the percent reduction of area. In addition, the appearance of the fracture surfaces is noted.

Since the electrodes were purchased to meet the AWS-ASTM designations E7016 and E6010, the tensile strength of the weld metal produced by the E7016 electrode was expected to be greater than the tensile strength of the weld metal produced by the E6010 electrode. However, the results of the tensile tests show that the strengths of the two weld metals were about the same. For the preheated condition, both types of weld metal had a yield point of about 57,000 psi. and a maximum nominal strength of 70,000 psi. When quenched two minutes after welding, the strength increased for both electrodes, the nominal yield point to about 63,000 psi and the maximum nominal strength to about 75,000 psi.

Although the properties of maximum nominal strength and nominal yield point were about the same for the two types of weld metal, the percent reduction of area and the percent elongation were considerably greater for the E7016 weld metal. For example, in the preheated condition, the reduction of area was 68 percent for the E7016 weld metal and 36 percent for the E6010 metal; and in the quenched condition, the reduction of area was 61 percent for the E7016 weld metal and 19 percent for the E6010 weld metal. The same trend is indicated by the percent elongation. The results also indicate that the reduction of area of the quenched E7016 weld metal is only 7 percent less than that of the preheated E7016 weld metal, whereas the reduction of area of the quenched E6010 weld metal is approximately half as great as that of the preheated E6010 weld metal.

The comparison of the two types of weld metal is facilitated by the stress-strain diagrams shown in Fig. 21. In this figure both a nominal stress-strain curve and a true stress-true strain curve are presented for both types of weld metal subjected to the preheated or to the quenched conditions. In the nominal stress-strain diagram, the differences in the strength and the ductility of the two types of weld metal can be noted, and the higher energy absorbing capacity of the E7016 weld metal is readily apparent. It was not possible to determine the maximum true stresses nor the maximum true strains; therefore, only the lower portion of the true stress-true strain curves can be plotted. Accordingly, neither the maximum true stresses nor maximum true strains for the different specimens can be compared. However, the region of stress covered in the true stress-true strain diagram includes the stresses to which the fatigue specimens were loaded.

The appearance of the fracture has been noted in Table 12 for all specimens, and typical photographs are shown in Fig. 22.

With the exception of one specimen (60AT9) which appeared to contain a defect, all of the preheated E7016 weld specimens had ductile cup-cone type fractures. In the quenched condition, the fracture surface of the E7016 specimens appeared to be rough and quite porous, containing numerous small holes. Other larger defects were also apparent.

The preheated E6010 specimens all contained gas pockets in the fracture surface, but otherwise had a ductile appearance. In the

quenched condition, however, the E6010 specimens not only contained gas pockets, but also contained numerous small, bright, cup-like surfaces which were oriented approximately perpendicular to the direction of the applied stress. These small defects, which are clearly shown in the photographs of Fig. 22, gave the fracture a very rough appearance similar to the rough tensile fracture area of the quenched E6010 type A fatigue specimens.

17. Results of Tensile Tests of Transverse Type DT Plain Plate Specimens and Transverse Type BT Weld Specimens

The results for the transverse type DT plain plate specimens are summarized in Table 13, and typical fracture surfaces are shown in Fig. 23. The plate material, which was stressed transversely to the direction of rolling, had a yield point of 35,000 psi, a maximum strength of 61,000 psi, and a reduction of area of 49 percent. The nominal stress-strain curve is shown in Fig. 24.

All of the transverse Type BT specimens, containing weld metal, heat-affected zone, and base metal, failed in the base metal. The results reported in Table 14 indicate that there were two distinct yield points; one at about 37,000 psi corresponded to the yield point of the base metal, and another, a higher yield point, corresponded to the yield point of the weld metal. The magnitude of the higher yield point, which ranged between 52,000 and 65,000 psi, was dependent on the type of electrode and on whether the specimen was preheated or quenched. Because fracture occurred in the base plate, the tensile

strength and ductility (reduction of area) of these specimens is approximately equal to the tensile strength and ductility of the base plate specimens.

Since the nominal strain is an average along the entire gage length, it does not represent the strain at any one region of the specimen. The nominal stress-strain diagram is shown in Fig. 24 to indicate the double yield point only.

All of the fractures of the BT and DT specimens (see Fig. 23) occurred in the base metal and the fracture surfaces contained the striations characteristic of failure in the base material.

V. SUMMARY AND CONCLUSIONS

18. SUMMARY

The purpose of the present investigation is to determine and to compare, quantitatively, the fatigue and the static properties of weld metal deposited by a low hydrogen E7016 electrode and by a high cellulose E6010 electrode.

Four series of fatigue tests were performed. In Series A, the specimens were machined entirely from weld metal and were stressed longitudinally, parallel to the direction of welding. In both Series B and Series C, the specimens were stressed transversely to the direction of welding and contained weld metal, heat-affected zone, and base metal. The Series B specimens had the weld metal centered in the test section with the fusion lines outside of the test section, whereas the Series C specimens had the heat-affected zone in the test section. The Series D specimens were machined entirely from the base metal.

The specimens, which had a test section 3/8 in. in diameter and 1/4 in. long, were tested in axial tension with a stress cycle varying from a minimum tension of approximately 1000 psi to a maximum tension. The weldments prepared with each of the two types of electrode were subjected to one of two conditions: (1) preheating, or (2) water quenching two minutes after welding. The fatigue test results for the Series A, C, and the Series D specimens are summarized in the following table.

Specimen		Fatigue Strength $f_{100,000}$ nominal stress ksi	Fatigue Strength $f_{2,000,000}$ nominal stress ksi
Type A Longitudinal All-Weld-Metal			
E6010	Preheated	53	40
E6010	Quenched	53	40
E7016	Preheated	-	65
E7016	Quenched	69	58
Type C Transverse Weld			
E6010	Preheated	42-51	37-47
E6010	Quenched	44-56	40-52
E7016	Preheated	48-52	43-47
E7016	Quenched	-	51-53
Type D Transverse Plain Plate		-	43

Three series of specimens were tested to determine the static tensile properties of welds prepared in the same manner as those which were employed in the fatigue investigation: (1) the type AT longitudinal weld specimen, which contained only weld metal; (2) the type BT transverse weld specimen, which contained weld metal, heat-affected zone, and base metal; and (3) the type DT plain plate specimen, in which the base material was stressed transversely to the direction of rolling, as in the type BT specimen. The tensile specimens were axially loaded and had a 1/2 in. diameter with a 2 in. gage length. The results of the tensile tests are summarized in the following table.

Specimen type	yield point psi	tensile strength psi	percent elongation %	reduction of area %
Type AT, Longitudinal				
E6010 Preheated	57	70	25	37
E6010 Quenched	63	74	14	20
E7016 Preheated	57	69	35	67
E7016 Quenched	64	77	28	62
Type DT, Transverse				
Plain Plate	36	61	31	49

19. CONCLUSIONS

Longitudinal Type A All-Weld-Metal Fatigue Tests

1. The fatigue strength of the E7016 weld metal was found to be significantly greater than the fatigue strength of the E6010 weld metal. In terms of the nominal stress, the fatigue strength for the preheated E7016 weld metal was approximately 25,000 psi greater than that of the preheated or the quenched E6010 weld metal. Similarly, the fatigue strength of the quenched E7016 weld metal was approximately 18,000 psi greater than the fatigue strength of the E6010 weld metal.

2. Gas pockets appeared to be the primary cause of the reduced fatigue strength of the E6010 weld metal. The fatigue strength of the quenched and of the preheated E6010 weld were about the same, fracture initiating at gas pockets in all cases. These gas pockets appeared to mask any difference in the fatigue behaviour of the quenched or of the preheated E6010 weld metal, which had a fatigue strength at 2,000,000 cycles of approximately 40,000 psi.

3. Polished specimens of preheated E7016 weld metal had a high resistence to repeated loads at stresses approaching the maximum nominal static strength of the material. For failure at 2,000,000 cycles, the fatigue strength was 65,000 psi nominal stress.

4. The E7016 weld metal quenched two minutes after welding had a fatigue strength about 7,000 psi nominal stress less than the fatigue strength of the preheated E7016 weld metal.

5. The fatigue failures of the quenched E7016 weld metal appeared to initiate at small defects.

Transverse Type C Weld Specimen Fatigue Tests

6. Except for the quenched E7016 specimens, the transverse weld specimens containing weld metal, heat-affected zone, and base plate had approximately the same fatigue strengths when prepared by the different welding procedures employed in these tests. The quenched E7016 specimens had a slightly higher resistance to fatigue.

7. Considerable scatter was noted in the test results for the Type C specimens, and hence, the results are reported in terms of a range of fatigue strength. The preheated and the quenched E6010 specimens and the preheated E7016 specimens had a fatigue strength for failure at 2,000,000 cycles in the range of 37,000-52,000 psi, whereas the quenched E7016 specimens had a fatigue strength for failure at 2,000,000 cycles of 51,000-53,000 psi.

8. The fatigue strength of the transverse weld specimens was not greatly different from that of the transverse plain plate specimens,

which had a fatigue strength for failure at 2,000,000 cycles of approximately 43,000 psi.

9. The fatigue failure of the Type C E6010 weld specimens originated at gas pockets for all but one specimen, which failed at a defect at or near the fusion line. The fractures of the E7016 specimens initiated either in the base plate or at defects at or near the fusion line.

Longitudinal Type AT All-Weld-Metal Tensile Tests

10. The results of the longitudinal all-weld-metal tensile tests showed that the yield points (57,000 psi nominal stress) and the ultimate strengths (70,000 psi nominal stress) of the preheated E6010 and the preheated E7016 weld metals were approximately the same. Similarly, in the quenched condition, the yield point and the ultimate strengths of the two types of weld metal were approximately equal, but increased to 63,000 psi and 75,000 psi, respectively.

11. The ductility of the E7016 weld metal is significantly greater than that of the E6010 weld metal for both the preheated and the quenched conditions.

12. All of the preheated E6010 weld specimens had gas pockets in the fracture surface; in addition to gas pockets, the fractures of the quenched E6010 weld metal contained numerous small, bright, cup-like surfaces. The quenched E7016 weld metal contained gas pockets and defects, and numerous small holes which made the fracture surface appear porous. Only one of the preheated E7016 weld specimens had a defect in its fracture surface.

Transverse Tensile Tests

13. All of the transverse weld tensile coupons, containing weld metal, heat-affected zone, and base metal, failed in the base metal. The base metal had a yield point of 35,000 psi and an ultimate strength of 61,000 psi. These values are both considerably lower than the corresponding values obtained from the longitudinal all-weld-metal tensile tests.

BIBLIOGRAPHY

1. Flanigan, A. E., "An Investigation of the Influence of Hydrogen on the Ductility of Welds in Mild Steel", Welding Journal, Vol. 26, No. 4, pp 193s to 214s, 1947

2. Flanigan, A. E., Bocarsky, S. I., and McGuire, G. B., "Effect of Low-Temperature Cooling Rate on the Ductility of Arc Welds in Mild Steel", Welding Journal, Vol. 29, No. 9, pp 459s to 466s, 1950

3. Flanigan, A. E., and Kaufman, M., "Microcracks and the Low-Temperature Cooling Rate Embrittlement of Welds", Welding Journal, Vol. 30, No. 12, pp 613s to 622s, 1951

4. Harris, L. A., Matthiesen, R. B., and Sinnamon, G. K., "Effects of Hydrogen and Related Variables on the Physical Properties of Welds on Structural Steels", Report to the Ohio River Division Laboratories, Corps of Engineers, U. S. Army, Contract DA-33-017-eng-96, Civil Engineering Studies, Structural Research Series No. 31, University of Illinois, Sept. 1952.

5. Carney, D. J., Chipman, J., and Grant, N. J., "The Tin-Fusion Method for the Determination of Hydrogen in Steel", Journal of Metals, Vol. 188, No. 2, pp 397s to 403s, Feb. 1950

TABLE 1

Tensile Properties of Plate Material

Spec.	Yield Point	Maximum Strength	Reduction of Area	Elongation
	ksi	ksi	percent	percent
B89B1	34.7	61.0	55	29
B89C1	35.2	61.2	56	32

TABLE 2

Chemical Composition of Plate Material

Spec.	Composition in percent				
	Carbon	Manganese	Phosphorus	Sulphur	Silicon
B87L	0.25	0.48	0.016	0.036	0.03

TABLE 3

Results of Chemical Analyses of Weld Pads

Electrode	Box No.	Composition in percent				
		Carbon	Manganese	Phosphorus	Sulphur	Silicon
E6010	11	0.10	0.79	0.023	0.033	0.21
	10	0.10	0.78	0.023	0.032	0.21
	9	0.09	0.76	0.024	0.033	0.19
	8	0.10	0.78	0.024	0.033	0.18
E7016	13	0.12	0.51	0.025	0.029	0.39
	12	0.12	0.55	0.026	0.031	0.41
	11	0.10	0.51	0.025	0.028	0.37
	10	0.11	0.52	0.025	0.027	0.38

TABLE 4

Results of Hydrogen Analyses of Weld Pads

E6010		E7016	
Preheated (B91Q3) Parts per Million	Quenched (B91R3) Parts per Million	Preheated (B91S3) Parts per Million	Quenched (B91T3) Parts per Million
11.4	11.2	1.4	2.2
10.1	9.3	1.1	1.3
9.4	9.0	0.5	0.7

TABLE 5

Results of Hardness Surveys of Weld Cross-Sections

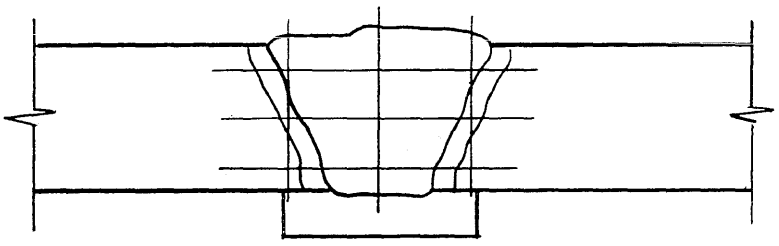

Specimen 00B45
E6010 Preheated

Region[a]	Average Vickers Hardness	Range	No. of Readings
BM	139	126-149	44
HAZ	145	129-164	25
WM	153	125-178	52
line 1	153	143-164	13
line 2	151	125-158	10
line 3	148	137-156	10
BUS	117	111-127	3

Specimen 60B41
E7016 Preheated

Region[a]	Average Vickers Hardness	Range	No. of Readings
BM	156	134-179	38
HAZ	157	142-177	29
WM	169	147-198	51
line 1	178	169-190	12
line 2	169	160-178	11
line 3	153	147-163	8
BUS	126	125-127	2

Specimen 02B55
E6010 Quenched

Region[a]	Average Vickers Hardness	Range	No. of Readings
BM	157	132-182	47
HAZ	174	161-192	15
WM	185	163-225	46
line 1	184	180-191	12
line 2	190	177-202	10
line 3	174	163-180	8
BUS	122	119-125	3

Specimen 62B51
E7016 Quenched

Region[a]	Average Vickers Hardness	Range	No. of Readings
BM	148	132-167	22
HAZ	161	149-194	18
WM	167	146-188	52
line 1	166	156-188	13
line 2	166	154-179	10
line 3	172	168-178	8
BUS	116	114-120	3

a
BM - Base Metal
WM - Weld Metal
HAZ - Heat-Affected Zone
BUS - Back-up Strip

TABLE 6

List of Specimens

Weld Spec.	Test Spec.	Test
B84A	62A5	fatigue
B84B	62AT10	tensile
B84C1	60B33	--
C2	60B19	fatigue
C3	60B23	fatigue
C4	60BT19	tensile
B84D	60A2	fatigue
B84E	62A0	fatigue
B84F	62A39	fatigue
B84G	02A13	fatigue
B84H	02A18	fatigue
B84J	00A6	fatigue
B84K1	00B38	--
K2	00B7	fatigue
K3	00B22	fatigue
K4	00BT17	tensile
B84L	02A46	fatigue
B84M	02AT12	tensile
B84N	00AT11	tensile
B84P	00A34	fatigue
B84Q1	02BT18	tensile
Q2	02B8	fatigue
Q3	02B20	fatigue
Q4	02B32	--
B84R	02A9	fatigue
B84S	00A1	fatigue
B84T1	00CT25	--
T2	00C31	fatigue
T3	00C49	fatigue
T4	00C65	fatigue
B84U	60A10	fatigue
B84V	60AT9	tensile
B84W	62A15	fatigue
B84X1	62BT20	tensile
X2	62B21	fatigue
X3	62B24	fatigue
X4	62B35	--
B84Y	60A14	fatigue
B84Z1	60CT27	--
Z2	60C37	fatigue
Z3	60C56	fatigue
Z4	60C61	--

Weld Spec.	Test Spec.	Test
B85A1	00B45	hardness
A2	00BT21	tensile
A3	00B52	crack
A4	00B60	--
B85B	00A63	fatigue
B85C	02AT16	tensile
B85D1	02C42	fatigue
D2	02C50	fatigue
D3	02C57	fatigue
D4	02CT26	--
B85E	60AT13	tensile
B85F	60A59	fatigue
B85G	62A53	fatigue
B85H1	62C36	fatigue
H2	62C43	fatigue
H3	62C62	fatigue
H4	62CT28	--
B85J	00A27	fatigue
B85K	00A28	fatigue
B85L	00A25	fatigue
B85M	00A26	fatigue
B85N	00A12	fatigue
B85P	00AT15	tensile
B85Q	02A3	fatigue
B85R1	02B40	crack
R2	02B55	hardness
R3	02BT22	tensile
R4	02B64	--
B85S	00A16	fatigue
B85T	02A58	fatigue
B85U	60A4	fatigue
B85V	60A17	fatigue
B85W1	62B44	--
W2	62B51	hardness
W3	62BT24	tension
W4	62B47	crack
B85X	62A11	fatigue
B85Y1	60B41	hardness
Y2	60BT23	tensile
Y3	60B48	crack
Y4	60B54	--
B85Z	62AT14	tensile

Weld Spec.	Test Spec.	Test
B91A	00A29	--
B91B	00A30	--
B91F1	BXB1	fatigue
F2	BXB2	fatigue
F3	BXB3	fatigue
F4	BXB4	tensile
B91P1	BXB5	fatigue
P2	BXB6	fatigue
P3	BXB7	tensile
P4	BXB8	fatigue
B91Q1	00C69	fatigue
Q2	00C77	fatigue
Q3		hyd. anal.
Q4	00C74	fatigue
B91R1	0ZC67	fatigue
R2	0ZC70	fatigue
R3		hyd. anal.
R4	02C73	fatigue
B91S1	60C76	fatigue
S2	60C66	fatigue
S3		hyd. anal.
S4	60C71	fatigue
B91T1	62C72	fatigue
T2	62C75	fatigue
T3		hyd. anal.
T4	62C68	fatigue
B86KL	60T1	tensile
B86MN	60T2	tensile
B86PQ	60T3	tensile
B86RS	60T4	tensile
B90HJ	00T5	tensile
B90KL	00T6	tensile
B90MN	00T7	tensile
B90PQ	00T8	tensile

TABLE 7

RESULTS OF FATIGUE TESTS OF LONGITUDINAL ALL-WELD-METAL SPECIMENS - SERIES A

Spec.	Yield Point ksi	Maximum Stress Nom. ksi	Maximum Stress True ksi	Cycles to Failure 1000's	Observations of Fracture Surface
					E6010 Preheated
00A1	49.5	56.5	56.8	74	Failure started at internal gas pocket - gas pocket in ductile tensile fracture
00A6	--	50.7	50.7	160	Failure started at internal gas pockets on two levels - gas pocket in ductile tensile fracture
00A12	--	47.6	47.6	2289[a]	Did not fail
00A34	--	49.0	49.0	133	Failure started at internal gas pocket - ductile tensile fracture
00A63	--	46.9	46.9	148	Failure started at internal gas pockets - gas pocket in ductile tensile fracture
					E6010 Quenched Two Minutes After Welding
02A3	--	43.6	43.7	1304	Failure started at internal gas pocket - many small bright surfaces in tensile fracture
02A9	--	54.9	54.9	57	Failure started at internal gas pocket - many small bright surfaces in tensile fracture
02A13	--	52.8	52.8	106	Failure started at gas pockets on two levels - small bright surfaces and one gas pocket in tensile fracture
02A18	--	43.9	43.9	330	Failure started at gas pocket - small bright surfaces in tensile fracture
02A46	--	43.2	43.2	455	Failure started at gas pocket at surface - many small defects in tensile fracture
02A58	--	52.2	52.3	211	Failure started at gas pocket at surface - many small defects in tensile fracture

[a] Did not fail

TABLE 7 (cont.)

RESULTS OF FATIGUE TESTS OF LONGITUDINAL ALL-WELD-METAL SPECIMENS - SERIES A

Spec.	Yield Point ksi	Maximum Stress Nom., ksi	Maximum Stress True ksi	Cycles to Failure 1000's	Observations of Fracture Surface
					E7016 Preheated
60A2	56.5	64.3	69.7	2009[a]	Did not fail
60A10	57.1	68.7	73.3	603	Failure started at small defect - ductile, shear-type tensile fracture
60A14	56.7	68.9	75.0	404	Failure started at surface - ductile, shear-type tensile fracture
60A17	62.7	66.7	71.9	875	Failure started at surface - ductile, shear-type tensile fracture
60A59	56.8	67.6	74.5	337	Failure started at surface - ductile, shear-type tensile fracture
					E7016 Quenched Two Minutes After Welding
62A0	64.5	70.1	70.8	85	Fracture marred on removal from testing machine
62A5	---	65.5	65.7	607	Failure started at internal defect - small bright spots in otherwise ductile appearing tensile fracture
62A11	---	64.7	64.8	153	Failure started at defect at surface - numerous small bright spots in otherwise ductile appearing tensile fracture
62A15	---	62.8	63.0	57	Failure started at surface, rough fracture surface - numerous small bright spots in otherwise ductile tensile fracture
62A39	---	62.0	62.0	420	Failure started at internal defect - numerous small bright spots in tensile fracture
62A53	68.5	68.5	71.2	63	Failure started at internal defect, rough fatigue fracture - bright spots in tensile fracture

[a] Did not fail.

TABLE 8

RESULTS OF FATIGUE TESTS OF LONGITUDINAL ALL-WELD-METAL SPECIMENS TO STUDY THE EFFECT OF WELDING VARIABLES

Spec.	Yield Point	Maximum Stress		Cycles to Failure	Observations of Fracture Surfaces
	ksi	Nom. ksi	True ksi	1000's	
					E6010 Preheated - OCV 88 volts - Electrode As-Stored
00A25	47.6	54.8	58.0	15	Failure started at internal gas pocket - two pockets in ductile, shear-type tensile fracture
00A26	47.3	52.6	54.9	40	Failure started at internal gas pocket - ductile, shear-type tensile fracture
					E6010 Preheated - OCV 66 volts - Electrode Dried
00A27	--	55.5	55.5	138	Failure started at internal gas pocket - ductile, shear-type tensile fracture
00A28	--	55.2	55.2	245	Failure started at internal gas pocket - ductile, shear-type tensile fracture
					E6010 Preheated - OCV 66 volts - Electrode Moistened
00A29	Not Tested				Gas pockets on exterior surface
00A30	Not Tested				Gas pockets on exterior surface

TABLE 9

RESULTS OF FATIGUE TESTS OF TRANSVERSE WELD SPECIMENS WITH WELD METAL CENTERED IN THE TEST SECTION - SERIES B

Spec.	Yield Point ksi	Maximum Stress Nom. ksi	Maximum Stress True ksi	Cycles to Failure 1000's	Observations of Fracture Surfaces
					E6010 Preheated
00B7	--	54.0	54.9	158	Failure started at gas pocket in weld metal, progressed into base metal - tensile fracture in both base metal and weld metal
00B22	--	48.8	48.5	204	Failure started at gas pocket at surface in weld metal - tensile fracture entirely in weld metal
					E6010 Quenched Two Minutes After Welding
02B8	--	54.5	54.6	85	Failure started at two gas pockets - numerous bright surfaces in tough tensile fracture
02B20	--	43.6	43.7	1072	Failure started at gas pocket at surface - numerous small bright surfaces in tensile fracture
					E7016 Preheated
60B19	55.5	65.8	71.4	201	Failure started from surface on two levels - appears to be at fusion line
60B23	58.1	62.5	66.8	189	Failure started from surface, progressed through both weld metal and base metal - striations in base metal tensile fracture
					E7016 Quenched Two Minutes After Welding
62B21	63.2	63.8	65.0	86	Failure started at defect near surface in weld metal
62B24	--	63.6	63.6	174	Failure started at gas pocket and defect, appears to be at fusion line - tensile fracture through both weld metal and base metal

TABLE 10

RESULTS OF FATIGUE TESTS OF TRANSVERSE WELD SPECIMENS WITH HEAT-AFFECTED ZONE CENTERED IN THE TEST SECTION - SERIES C

Spec.	Yield Point ksi	Maximum Stress Nom. ksi	Maximum Stress True ksi	Cycles to Failure 1000's	Observations of Fracture Surfaces
					E6010 Preheated
00C31	43.1	46.9	47.1	161	Failure started at gas pocket, second failure started on opposite side - two gas pockets in tensile fracture
00C49	--	43.3	43.3	528	Failure started at gas pocket - fracture entirely in weld metal - ductile tensile fracture
00C65	39.9	48.1	48.9	563	Failure started at internal gas pockets - gas pockets in ductile, shear-type tensile fracture
00C69	42.0	49.1	50.0	90	Failure started at gas pockets on several levels - fracture entirely in weld metal - ductile, shear-type tensile fracture
00C74	--	43.0	43.0	64	Failure started at gas pockets - fracture entirely in weld metal - ductile, shear-type tensile fracture
00C77	43.1	51.4	52.6	80	Failure started at gas pockets - fracture entirely in weld metal - ductile, shear-type tensile fracture
					E6010 Quenched Two Minutes After Welding
02C42	42.8	44.9	44.9	383	Failure started at defect, appears to be at fusion line - fracture in both weld metal and base metal - rough tensile fracture
02C50	43.1	50.3	50.7	334	Failure started at two gas pockets in weld metal - tensile fracture in both weld metal and base metal, striations in most of tensile fracture
02C57	43.1	53.8	54.0	287	Failure started at gas pockets on two levels - fracture entirely in weld metal - numerous bright spots in tensile fracture
02C67	43.9	43.8	43.9	222	Failure started at gas pockets in weld metal - fracture in both weld metal and base metal - gas pockets and bright spots in tensile fracture

TABLE 10 (cont.)

RESULTS OF FATIGUE TESTS OF TRANSVERSE WELD SPECIMENS WITH HEAT-AFFECTED ZONE CENTERED IN THE TEST SECTION - SERIES C

Spec.	Yield Point ksi	Maximum Stress Nom. ksi	Maximum Stress True ksi	Cycles to Failure 1000's	Observations of Fracture Surfaces
					E6010 Quenched Two Minutes After Welding
02C73	39.8	45.3	45.4	376	Failure started at gas pocket - fracture entirely in weld metal - gas pocket and small bright spots in tensile fracture
02C70	--	41.8	41.8	432	Failure started at gas pocket at fusion line - fracture in both weld metal and base metal - striations in rough tensile fracture
					E7016 Preheated
60C37	44.9	49.6	50.6	117	Failure started at defects near fusion line in weld metal, rough fatigue fracture - rough and striated tensile fracture
60C61	42.9	46.5	46.9	179	Failure started at group of small gas pockets in weld metal near fusion line - deep striations in tensile fracture
60C66	--	44.4	4.44	2956[a]	Did not fail
60C71	41.5	46.8	46.9	2349	Failure started from surface, entirely in base metal, light striations in fatigue fracture - deep striations in tensile fracture
60C76	40.8	49.1	51.0	461	Failure started at very small defect at surface in weld metal, flat smooth fatigue fracture - ductile tensile fracture
					E7016 Quenched Two Minutes After Welding
62C43	44.9	54.8	56.8	361	Failure started at surface - fracture entirely in base metal - deep striations in tensile fracture
62C62	48.6	55.4	55.7	60	Failure started at defect in weld metal, fatigue fracture rough - tensile fracture in base metal, deeply striated
62C68	43.8	52.3	52.9	1987	Failure started at surface, probably in base metal, light striations in fatigue fracture - deep striations in tensile fracture
62C72	42.4	52.8	52.9	2271	Failure started at surface, might be in base metal, light striations in fatigue fracture - deep striations in tensile fracture
62C75	45.9	54.1	55.7	447	Failure started at surface, probably in base metal, light striations in fatigue fracture - deep striations in tensile fracture

[a] Did not fail

TABLE 11

RESULTS OF FATIGUE TESTS OF TRANSVERSE PLAIN PLATE SPECIMENS - SERIES D

Spec.	Yield Point ksi	Maximum Stress Nom. ksi	Maximum Stress True ksi	Cycles to Failure 1000's	Observations of Fracture Surface
BXB1	38.0	46.0	49.6	388	Failure started at surface, light striations in fatigue fracture - deep striations in tensile fracture
BXB2	38.8	43.3	54.2	1050	Failure started at surface, light striations in fatigue fracture - deep striations in tensile fracture
BXB5	29.5	43.6	45.0	1381	Failure started at surface, light striations in fatigue fracture - deep striations in tensile fracture
BXB6	38.2	41.9	42.8	2501[a]	Did not fail
BXB8	37.7	45.1	47.2	1113	Failure started at surface, light striations in fatigue fracture - deep striations in tensile fracture

[a] Did not fail

TABLE 12

RESULTS OF TENSILE TESTS OF LONGITUDINAL ALL-WELD-METAL SPECIMENS - SERIES AT

Spec.	Yield Point ksi	Max. Nom. Stress ksi	Elong. percent	Red. of Area percent	Remarks
			E6010 Preheated		
00T5	---	69.7	27	33	Ductile, shear-type failure - 2 gas pockets
00T6	58.3	72.3	26	30	Ductile, shear-type failure - 3 gas pockets
00T7	58.3	70.4	25	34	Ductile, shear-type failure - 3 gas pockets
00T8	59.2	70.9	25	43	Ductile, shear-type failure - 3 gas pockets
00AT11	52.2	67.0	24	35	Ductile, shear-type failure - 4 gas pockets
00AT15	56.9	71.1	25	44	Ductile, shear-type failure - 1 gas pocket
			E6010 Quenched Two Minutes After Welding		
02AT16	62.4	73.0	14	21	Several gas pockets - numerous small, shiny, cup-like surfaces
02AT16	63.9	75.0	14	18	Several gas pockets - numerous small, shiny, cup-like surfaces
			E7016 Preheated		
60T1	58.1	69.4	35	68	Cup-cone failure, rough at base of cup
60T2	57.7	69.7	34	68	Cup-cone failure
60T3	59.2	70.3	36	68	Cup-cone failure
60T4	54.7	69.0	36	68	Cup-cone failure, rough at base of cup
60AT9	54.9	69.3	35	63	Ductile, shear-type failure - one defect
60AT13	55.0	68.3	37	70	Cup-cone failure
			E7016 Quenched Two Minutes After Welding		
62AT10	65.0	77.4	30	63	Porous appearance, many small holes - 1 gas pocket
62AT14	62.3	76.7	27	60	Porous appearance, small holes - 1 larger defect

TABLE 13

RESULTS OF TENSILE TESTS OF TRANSVERSE PLAIN PLATE SPECIMENS - SERIES DT

Spec.	First Yield Point ksi	Max. Nom. Stress ksi	Elong. percent	Red of Area percent	Remarks
BXB4	36	61	32	49	Rough, striated fracture
BXB7	36	62	29	49	Rough, striated fracture

TABLE 14

RESULTS OF TENSILE TESTS OF TRANSVERSE WELD SPECIMENS - SERIES BT

Spec.	First Yield Point ksi	Second Yield Point ksi	Max. Nom. Stress ksi	Elong percent	Red. of Area percent	Remarks
			6010 Preheated			
00BT17	39	53	64	23	46	Rough, striated fracture
00BT21	39	52	65	21	46	Rough, striated fracture
			6010 Quenched Two Minutes After Welding			
02BT18	34	57	65	16	45	Rough, striated fracture
02BT22	37	60	63	15	48	Rough, striated fracture
			7016 Preheated			
60BT19	38	52	64	23	47	Rough, striated fracture
60BT23	40	53	64	23	50	Rough, striated fracture
			7016 Quenched Two Minutes After Welding			
62BT20	35	64	64	16	49	Rough, striated fracture
62BT24	36	65	65	14	15	Rough, striated fracture

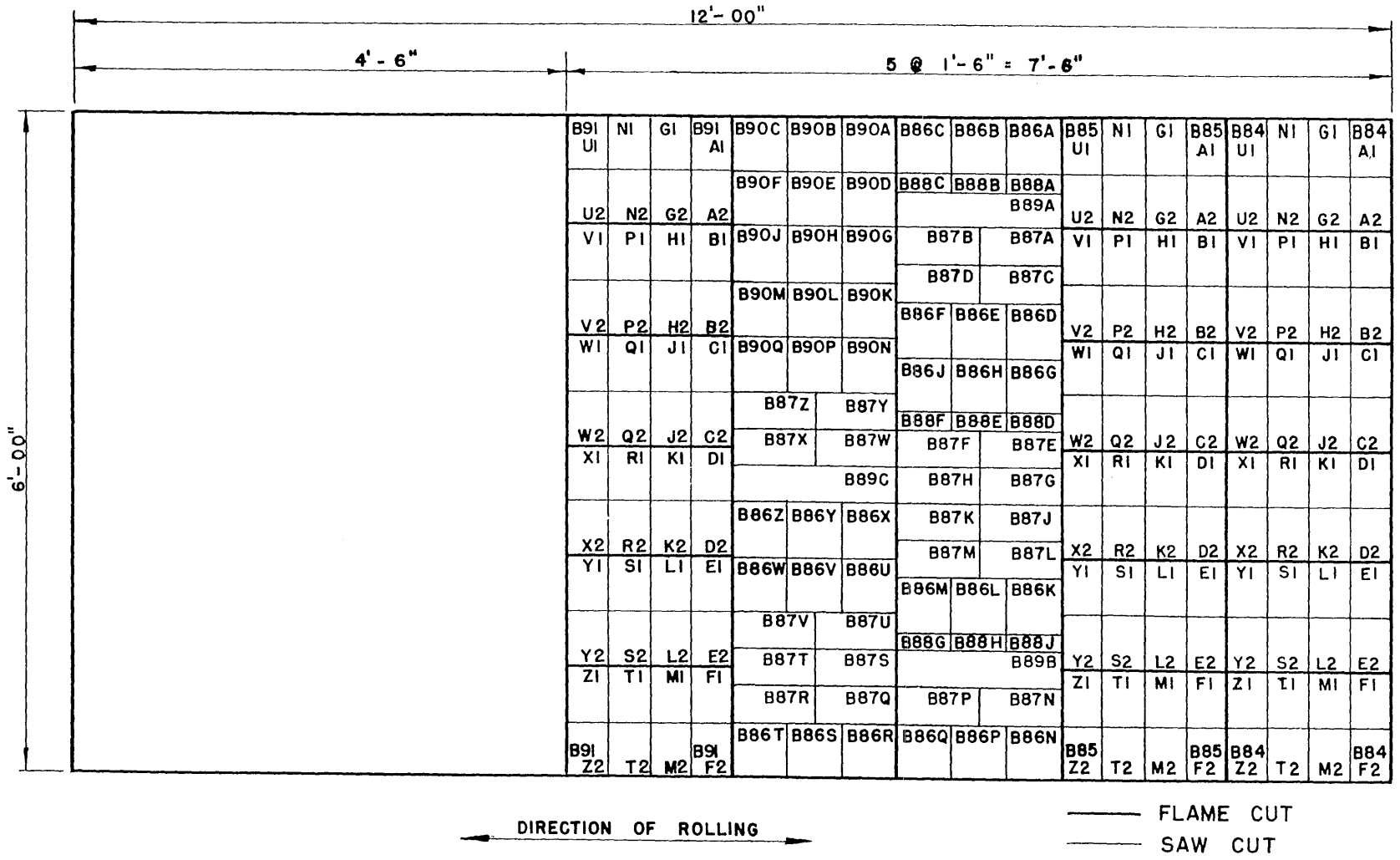

FIG. 1 LOCATION OF SPECIMENS IN PARENT PLATE

STEEL B, PLATE 4, 3/4 in.

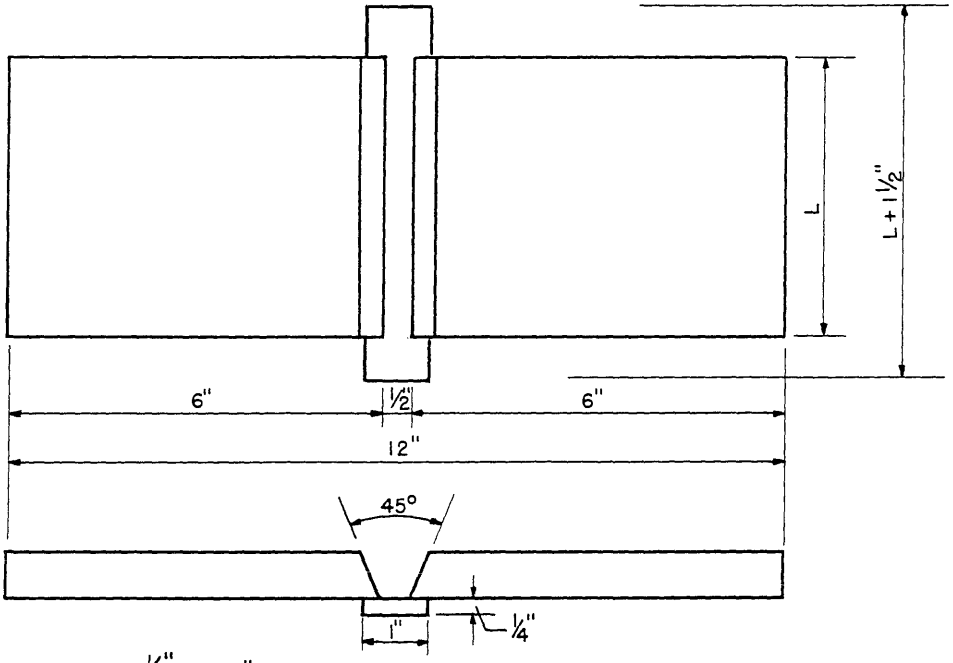

Note: L = 4½" or 6"

a. JOINT PREPARATION

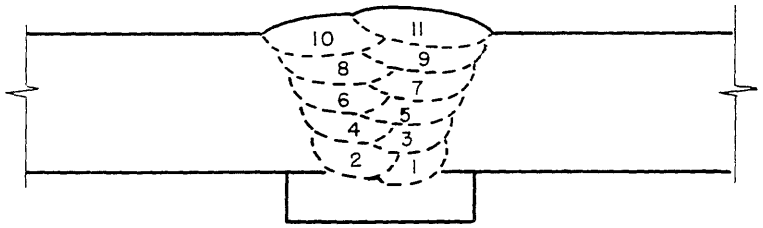

b. WELDING SEQUENCE

FIG. 2 DETAILS OF WELDMENTS

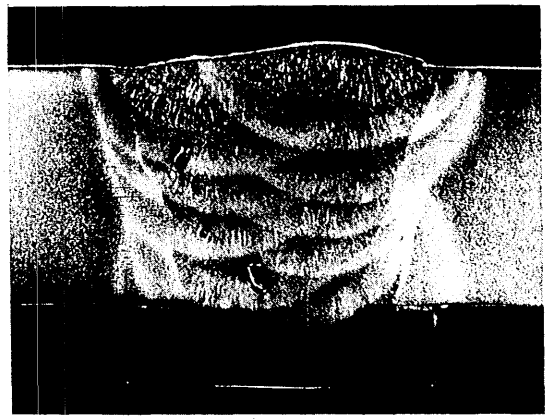

00B45

a. PREHEATED E6010

60B41

b. PREHEATED E7016

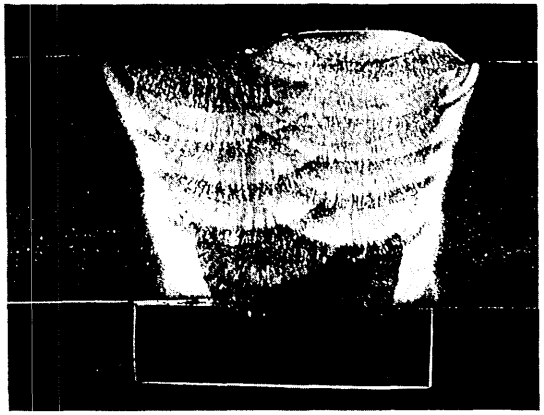

02B55

c. QUENCHED E6010

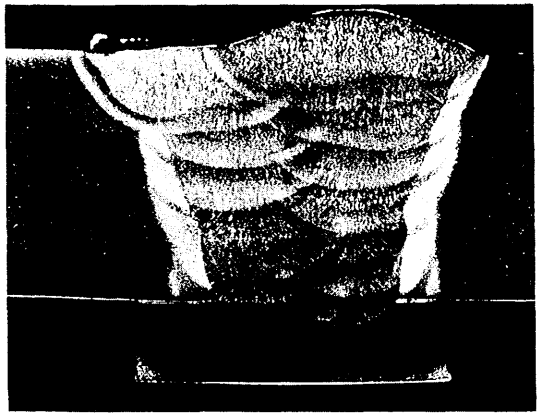

62B51

d. QUENCHED E7016

FIG. 3 MACRO-SECTIONS OF WELD PADS TRANSVERSE TO THE DIRECTION OF WELDING

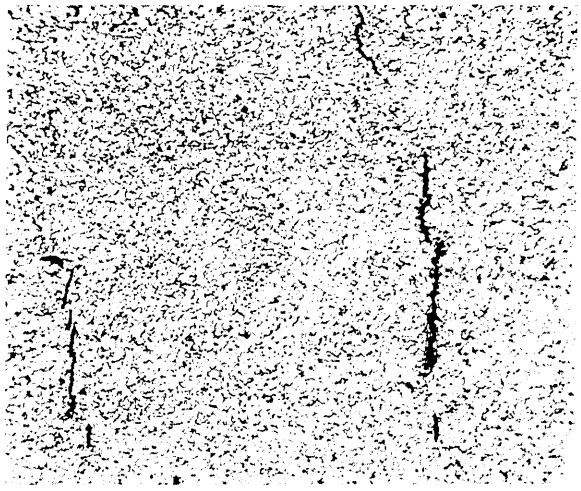

02B40

a. MICRO-CRACKS IN EQUIAXED ZONE NEAR MID-DEPTH OF QUENCHED E6010 WELD PAD MAGNIFICATION 150 X

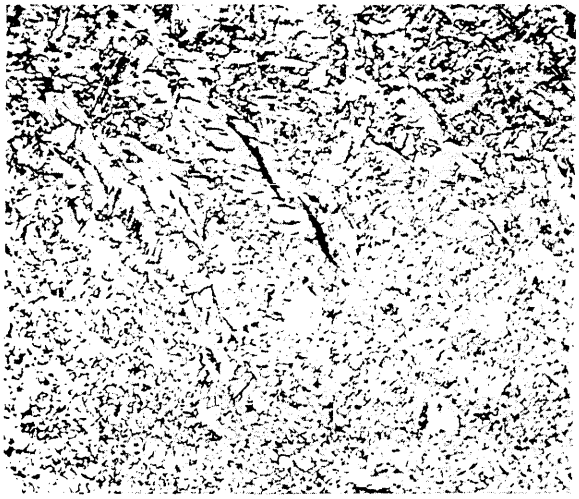

62B47

b. MICRO-CRACK IN DENDRITIC ZONE NEAR MID-DEPTH OF QUENCHED E7016 WELD PAD MAGNIFICATION 150 X

FIG. 4 MICRO-CRACKS IN WELD PADS WATER QUENCHED TWO MINUTES AFTER WELDING

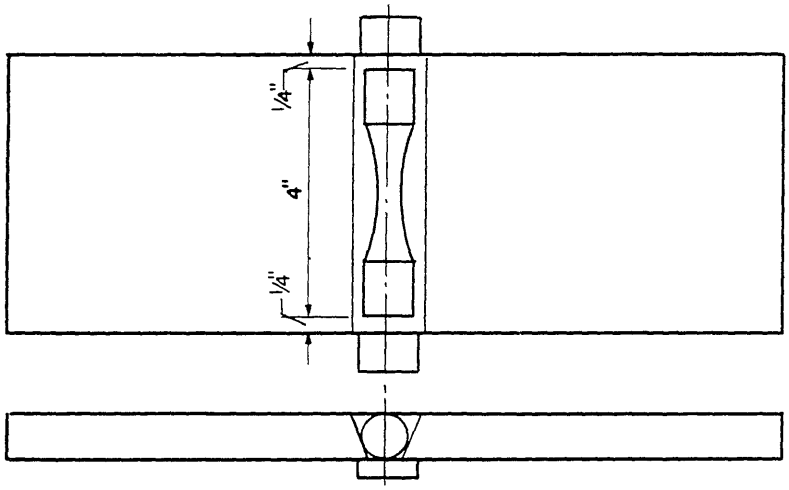

a. LONGITUDINAL ALL-WELD-METAL SPECIMEN – TYPE A

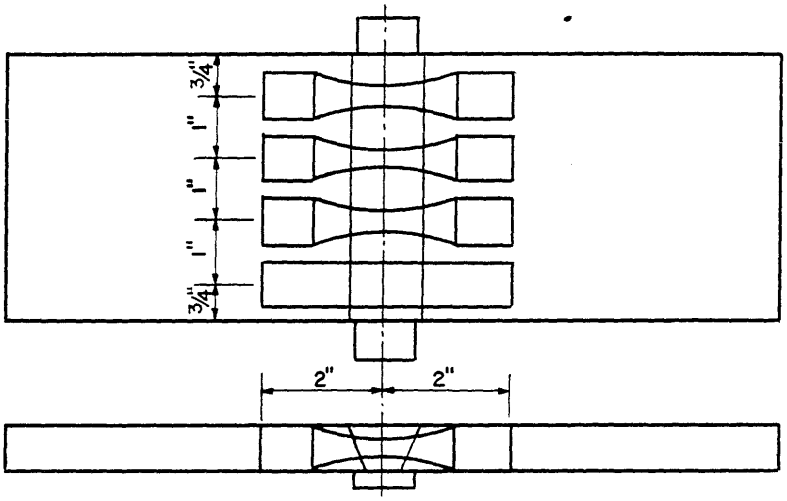

b. TRANSVERSE SPECIMENS WITH WELD METAL CENTERED IN TEST SECTION – TYPE B

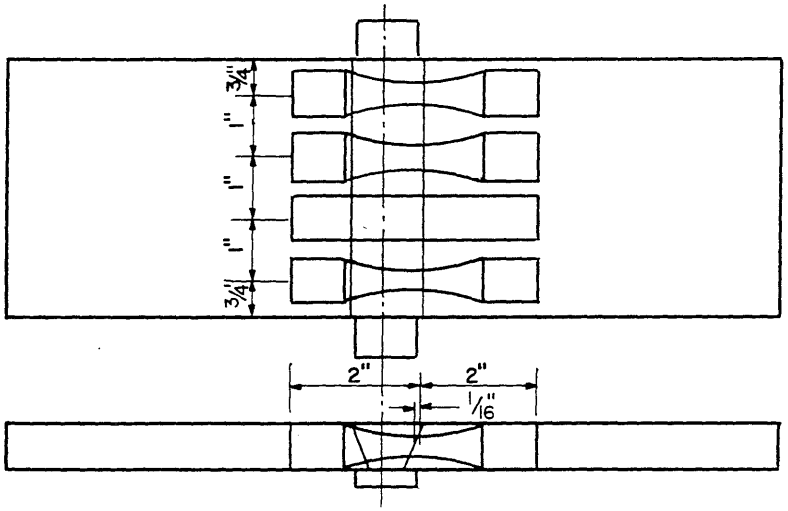

c. TRANSVERSE SPECIMENS WITH HEAT-AFFECTED ZONE CENTERED IN TEST SECTION – TYPE C

FIG. 5 LOCATION OF FATIGUE SPECIMENS IN WELDMENTS

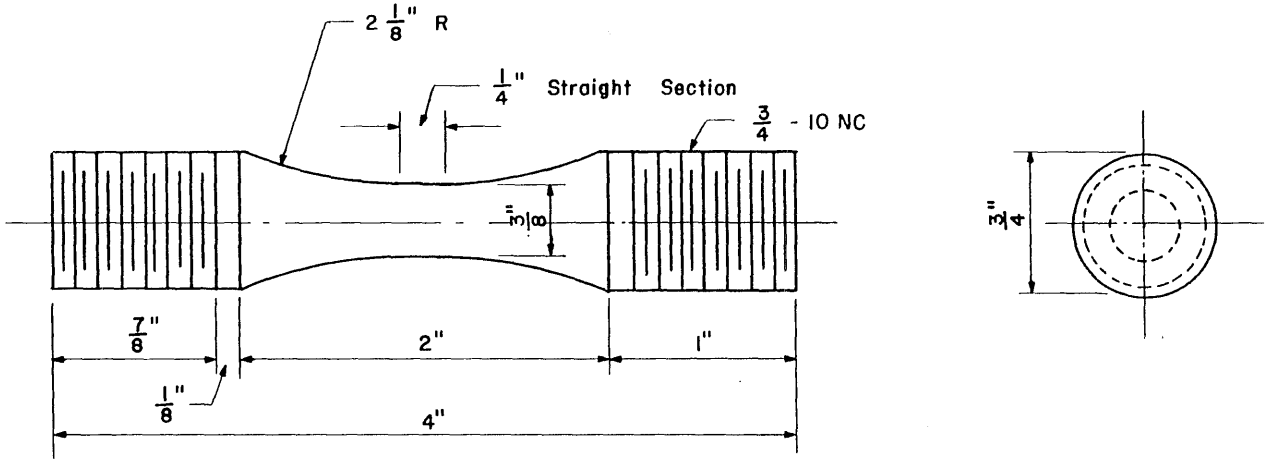

FIG. 6 DETAILS OF FATIGUE SPECIMENS

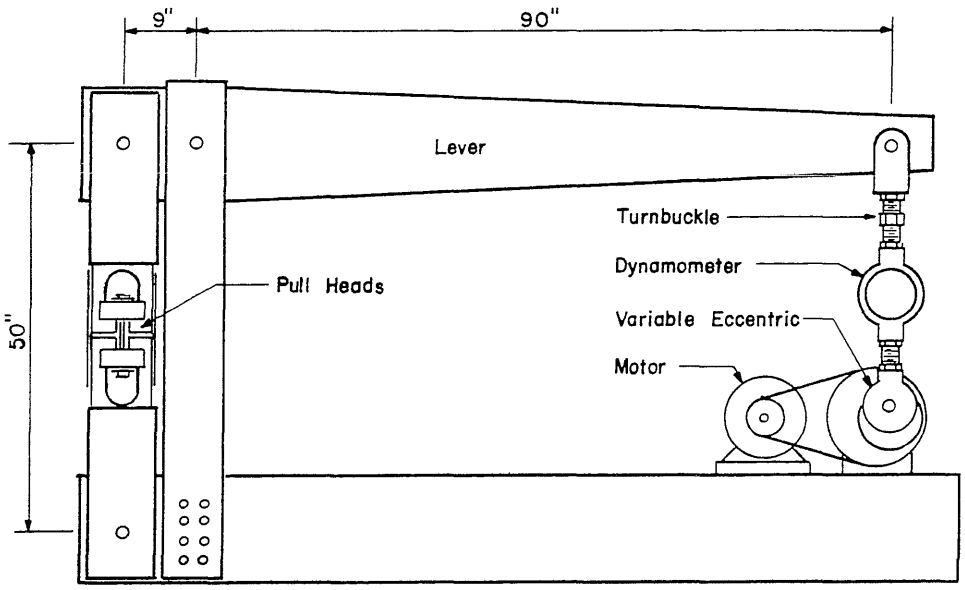

a. DIAGRAMATIC SKETCH OF WILSON FATIGUE TESTING MACHINE

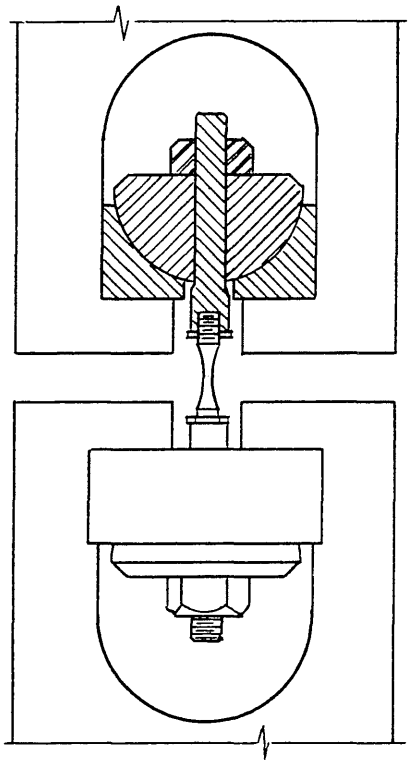

b. DETAIL OF SPHERICAL SEATS

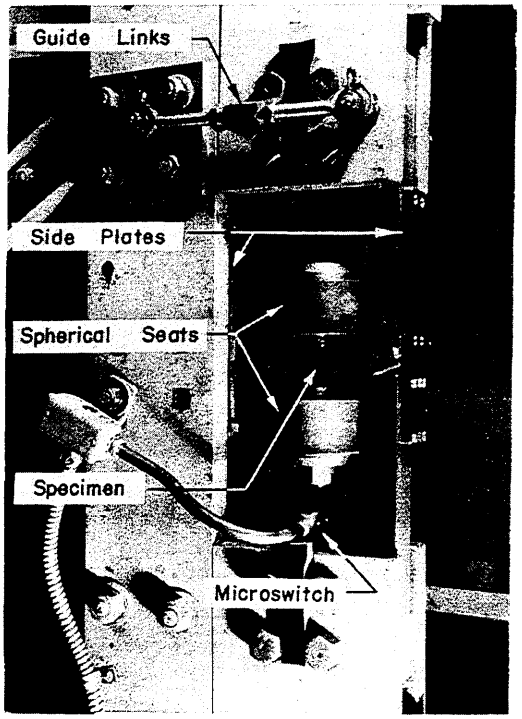

c. APPARATUS FOR MAINTAINING AXIAL LOAD

FIG. 7 WILSON FATIGUE MACHINE ADAPTED FOR SMALL AXIAL TESTS

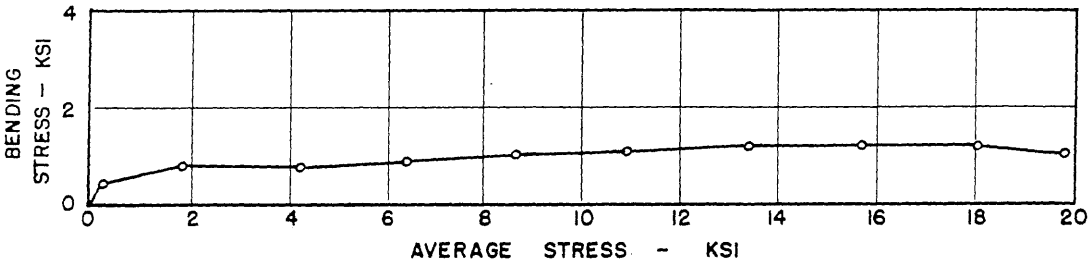

a. RELATIONSHIP BETWEEN BENDING STRESS AND AVERAGE STRESS

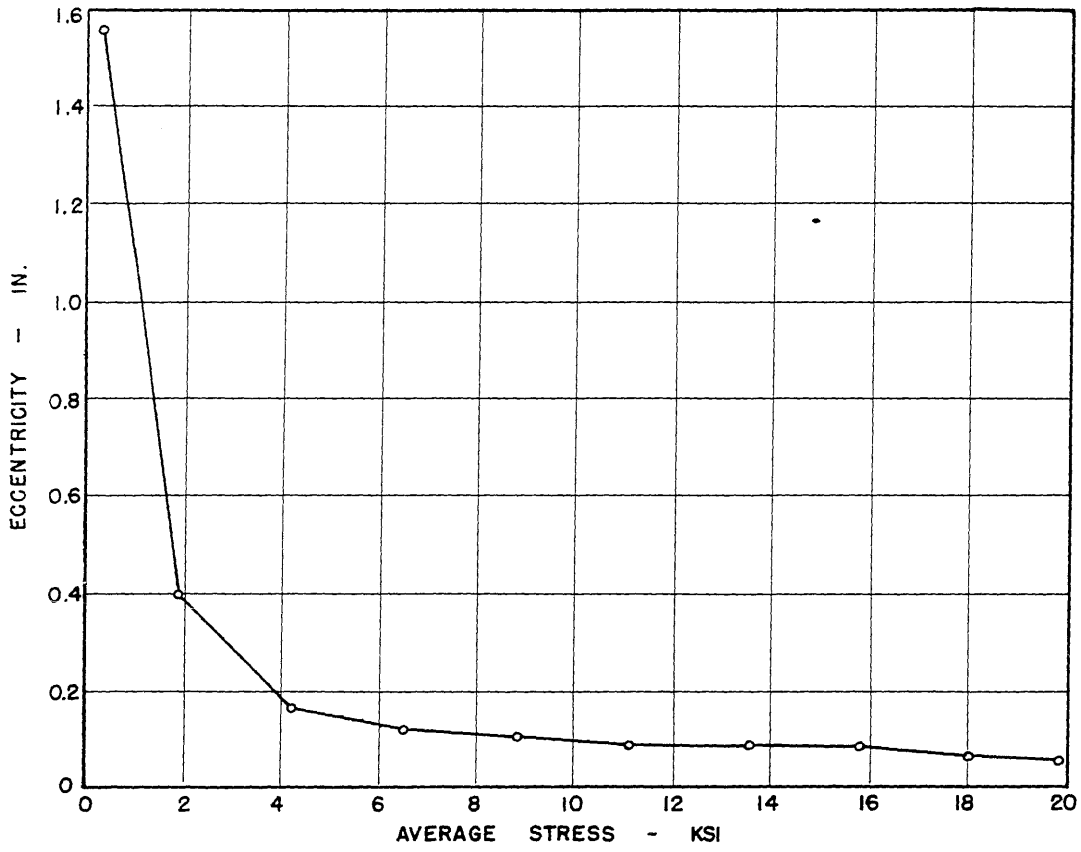

b. RELATIONSHIP BETWEEN ECCENTRICITY AND AVERAGE STRESS

FIG. 8 BENDING STRESS AND ECCENTRICITY AS FUNCTIONS OF AVERAGE STRESS ON 3/4 IN. DIAMETER CALIBRATION WEIGH BAR

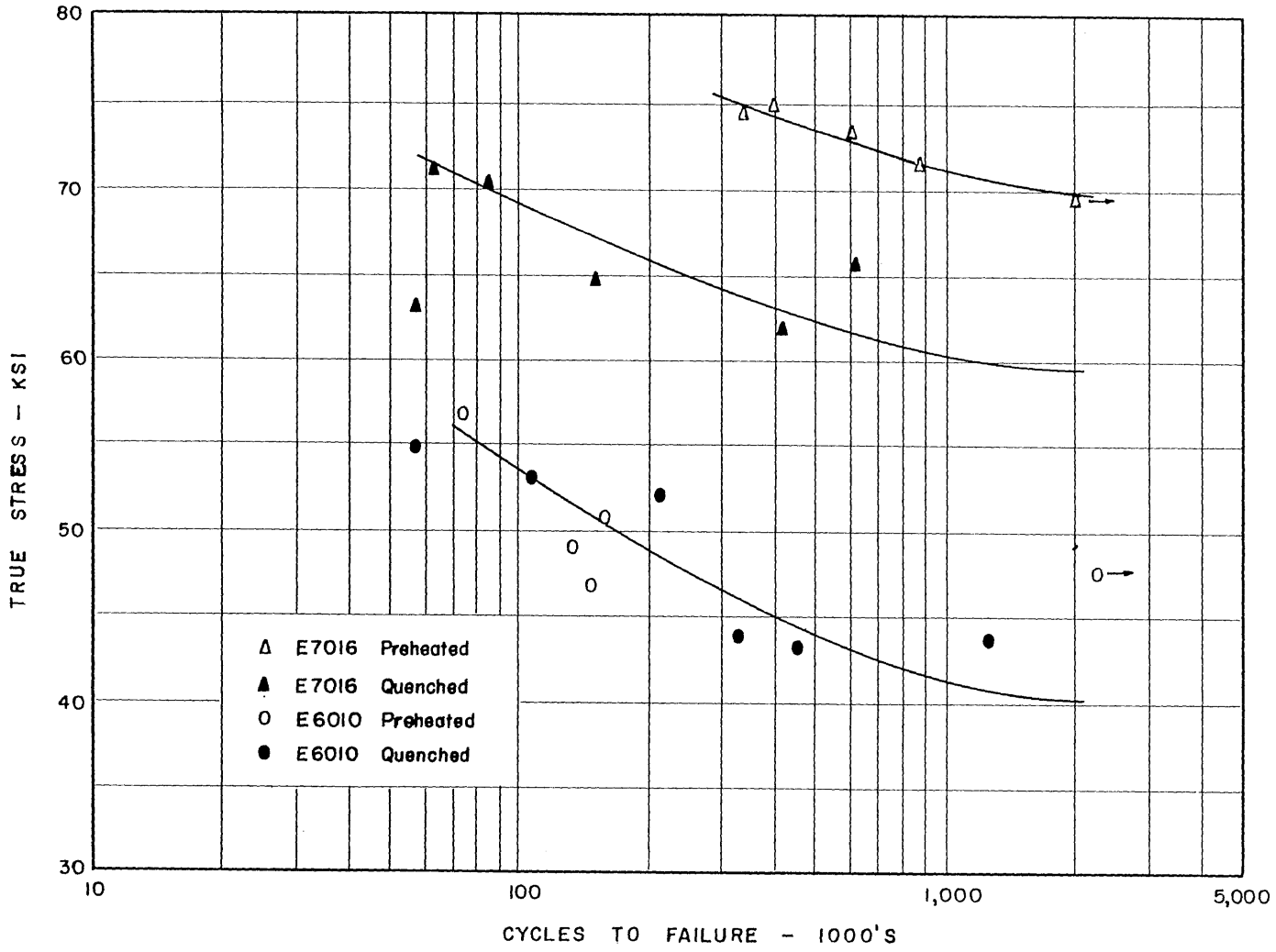

FIG. 9 RESULTS OF FATIGUE TESTS OF LONGITUDINAL TYPE A SPECIMENS IN TERMS OF TRUE STRESS

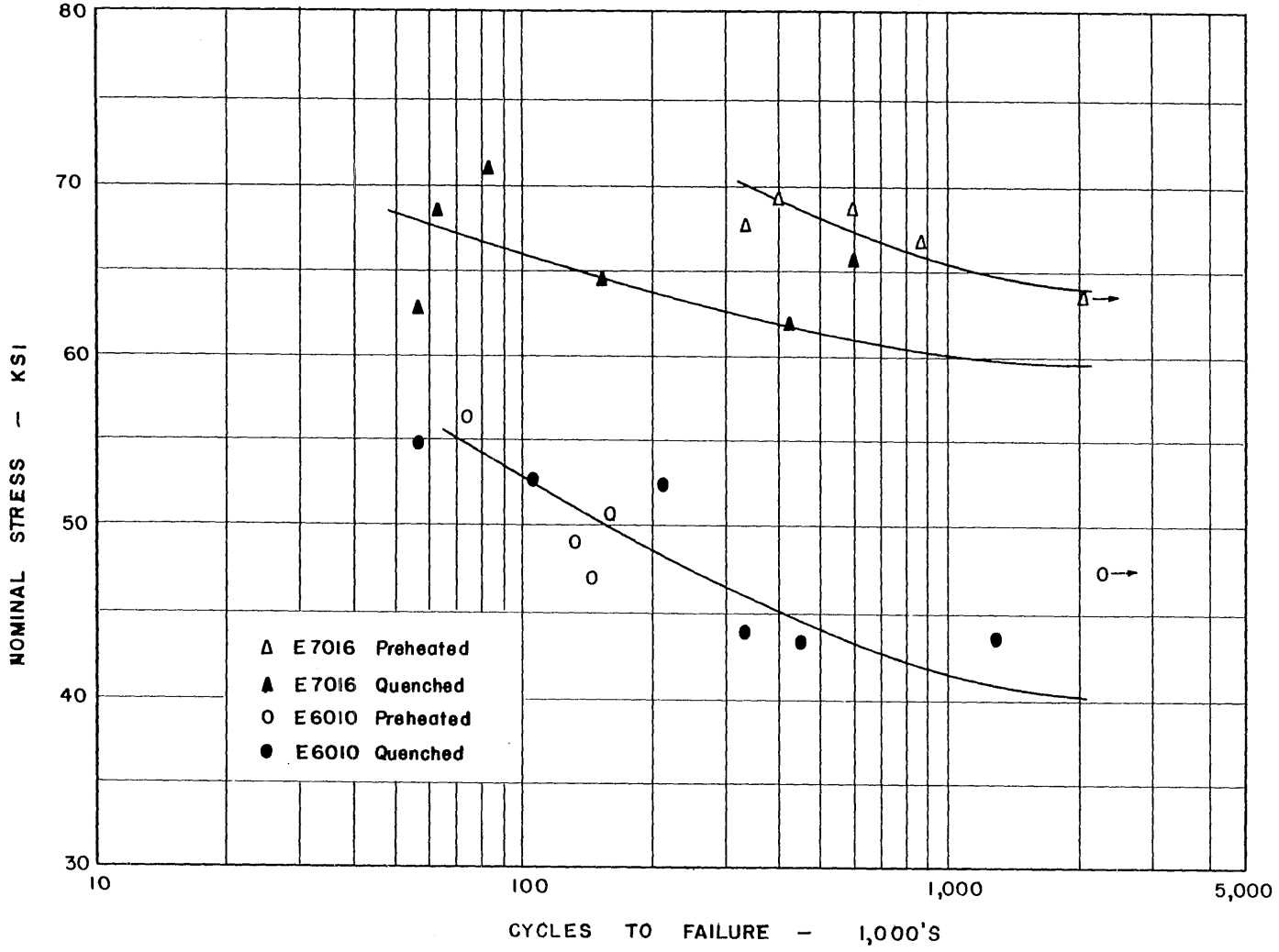

FIG. 10 RESULTS OF FATIGUE TESTS OF LONGITUDINAL TYPE A SPECIMENS IN TERMS OF NOMINAL STRESS

00A6

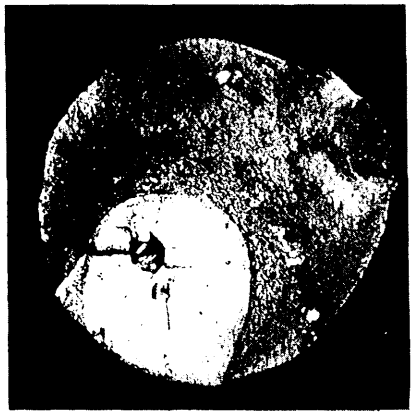

00A63

a. PREHEATED E6010

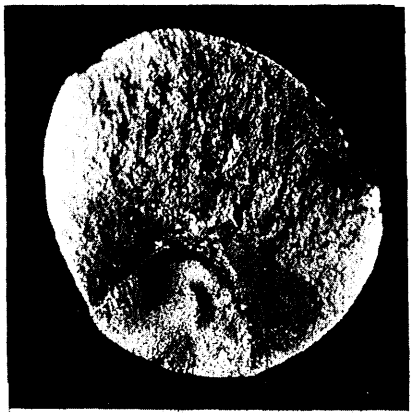

60A10

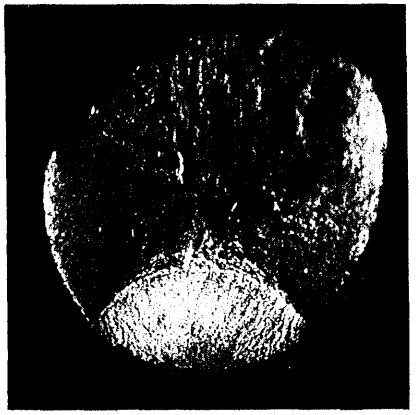

60A17

b. PREHEATED E7016

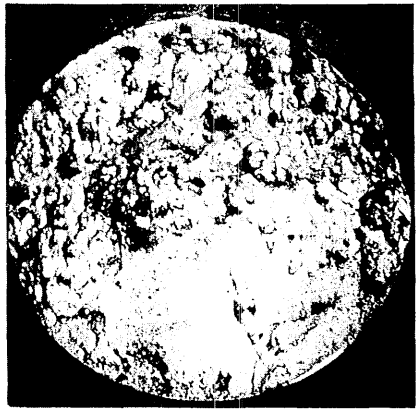

02A3

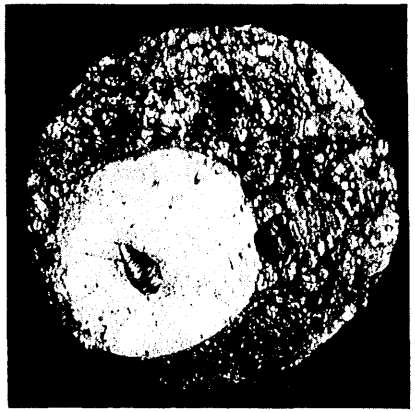

02A9

c. QUENCHED E6010

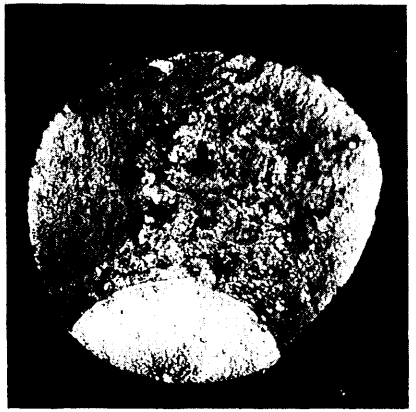

62A11

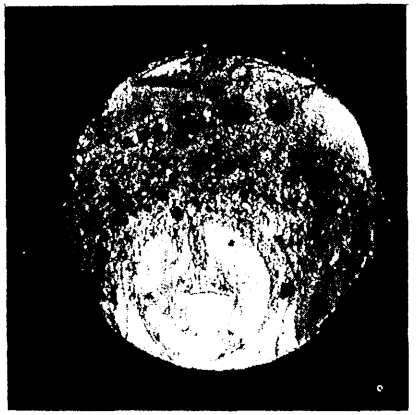

62A53

d. QUENCHED E7016

FIG. 11 PHOTOGRAPHS OF FRACTURE SURFACES OF LONGITUDINAL TYPE A FATIGUE SPECIMENS

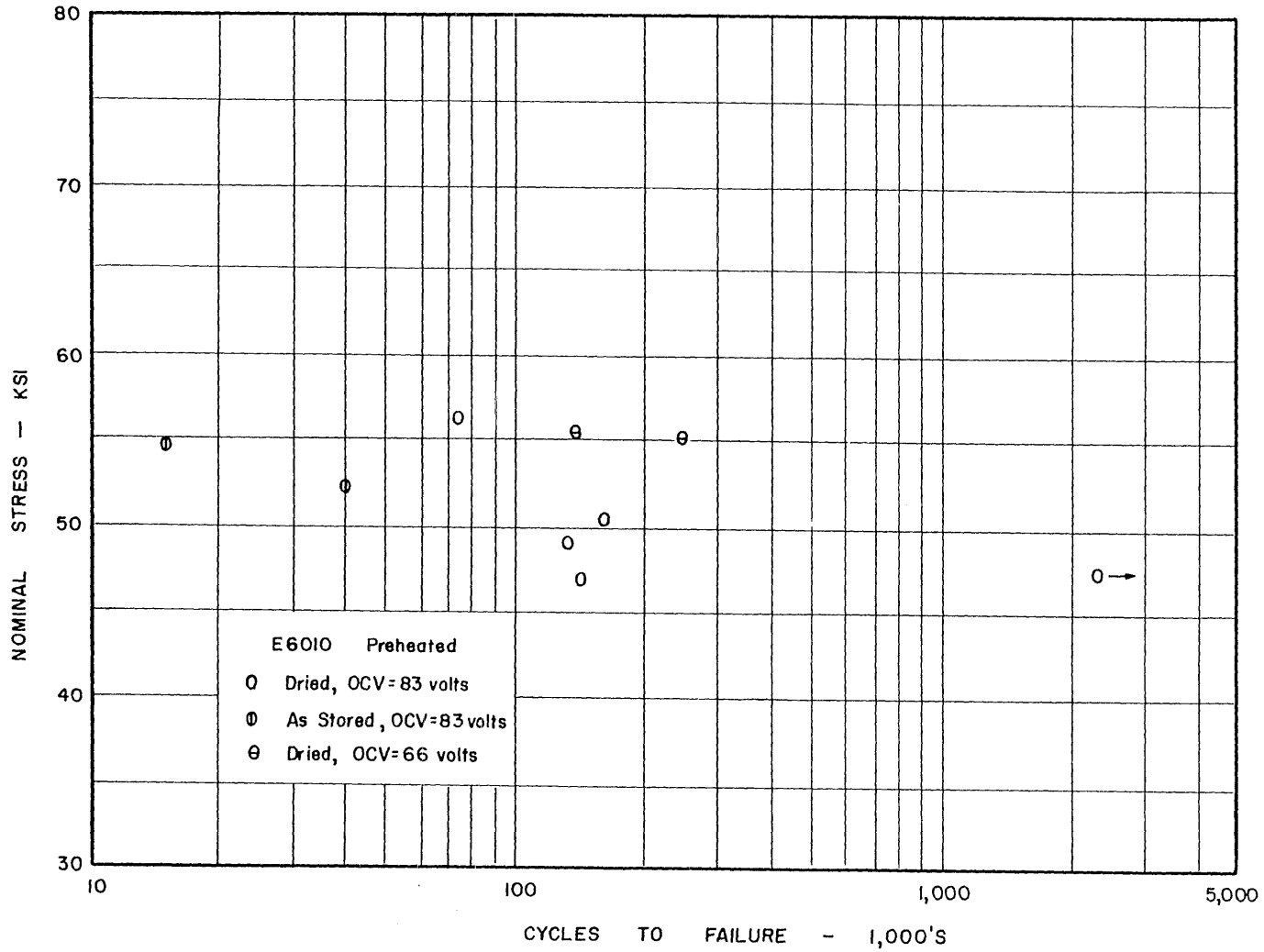

FIG. 12 RESULTS OF FATIGUE TESTS OF LONGITUDINAL TYPE A SPECIMENS TO STUDY THE EFFECT OF WELDING VARIABLES

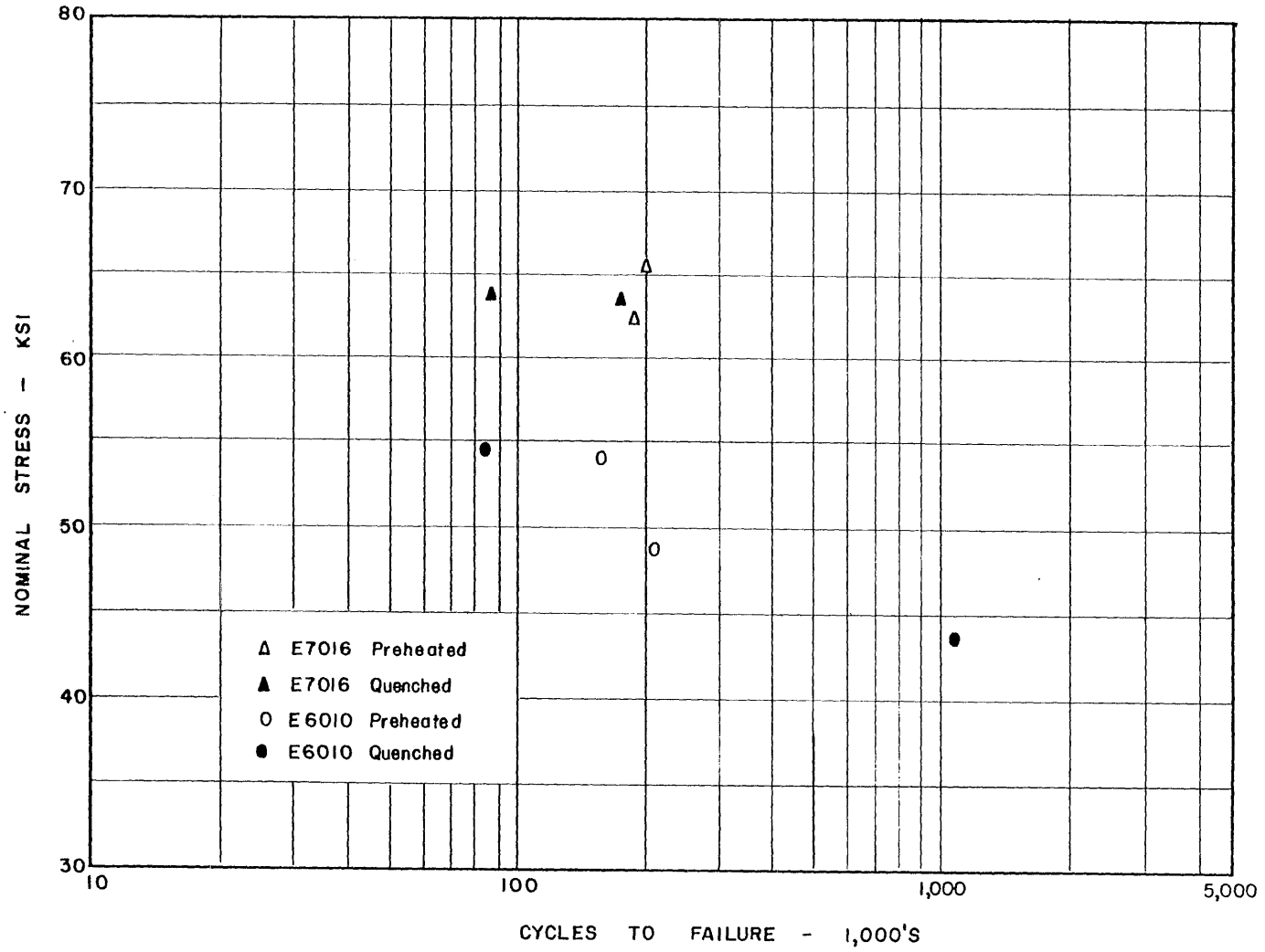

FIG. 13 RESULTS OF FATIGUE TESTS OF TRANSVERSE TYPE B SPECIMENS IN TERMS OF NOMINAL STRESS

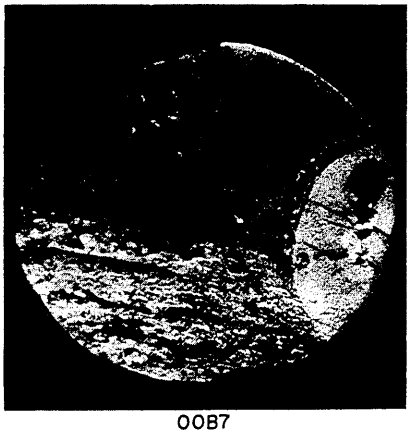

0087

a. PREHEATED E6010

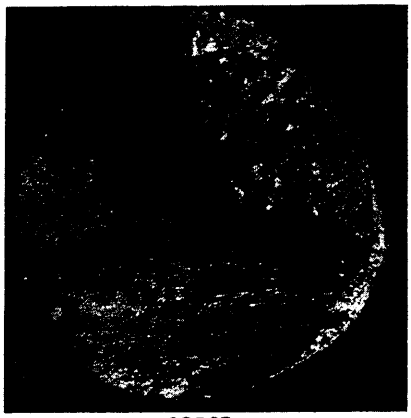

60B23

b. PREHEATED E7016

02B8

c. QUENCHED E6010

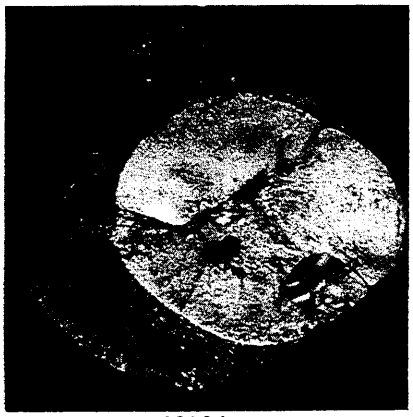

62B24

d. QUENCHED E7016

FIG. 14 PHOTOGRAPHS OF FRACTURE SURFACES OF TRANSVERSE TYPE B FATIGUE SPECIMENS

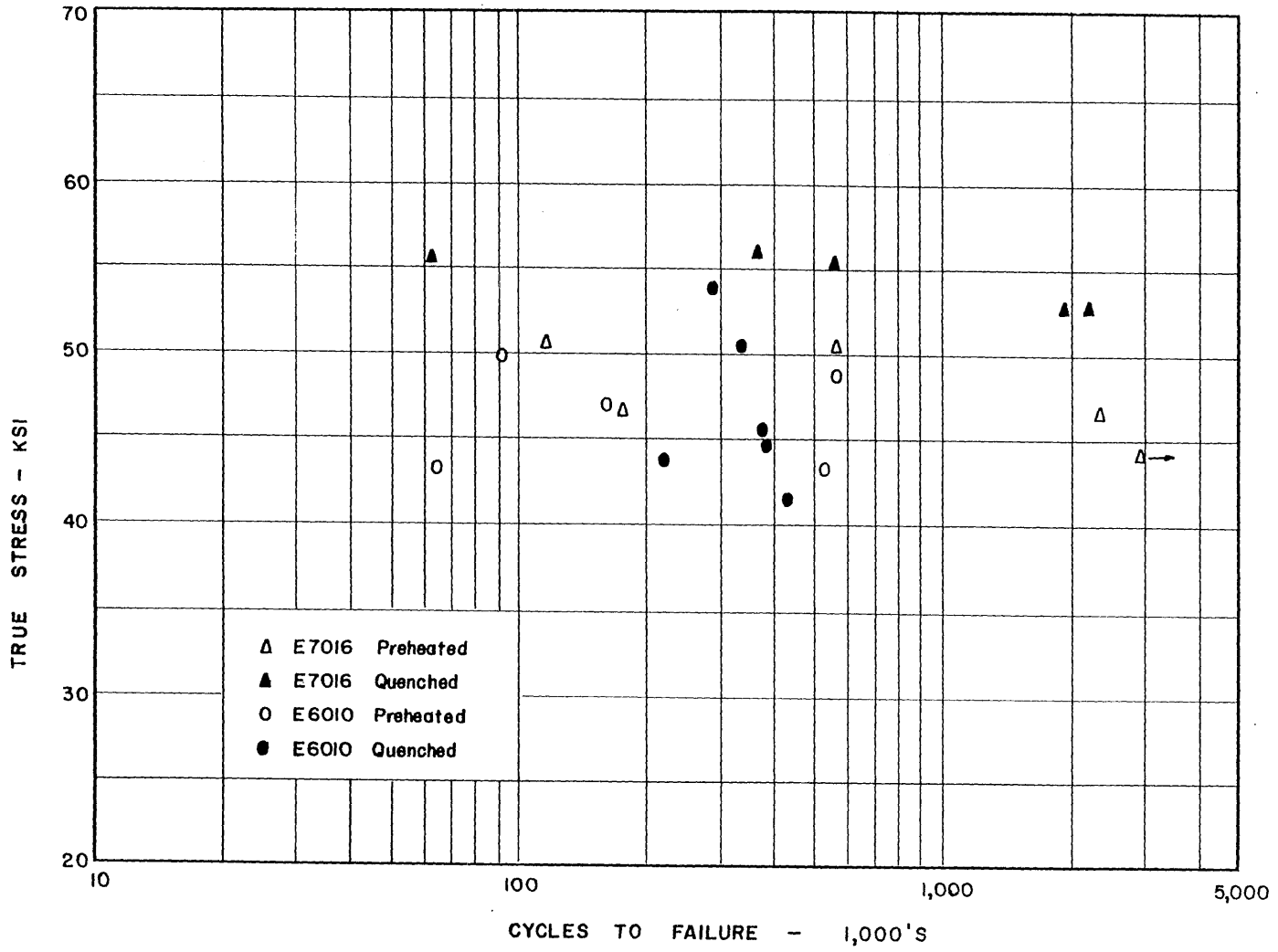

FIG. 15 RESULTS OF FATIGUE TESTS OF TRANSVERSE TYPE C SPECIMENS IN TERMS OF TRUE STRESS

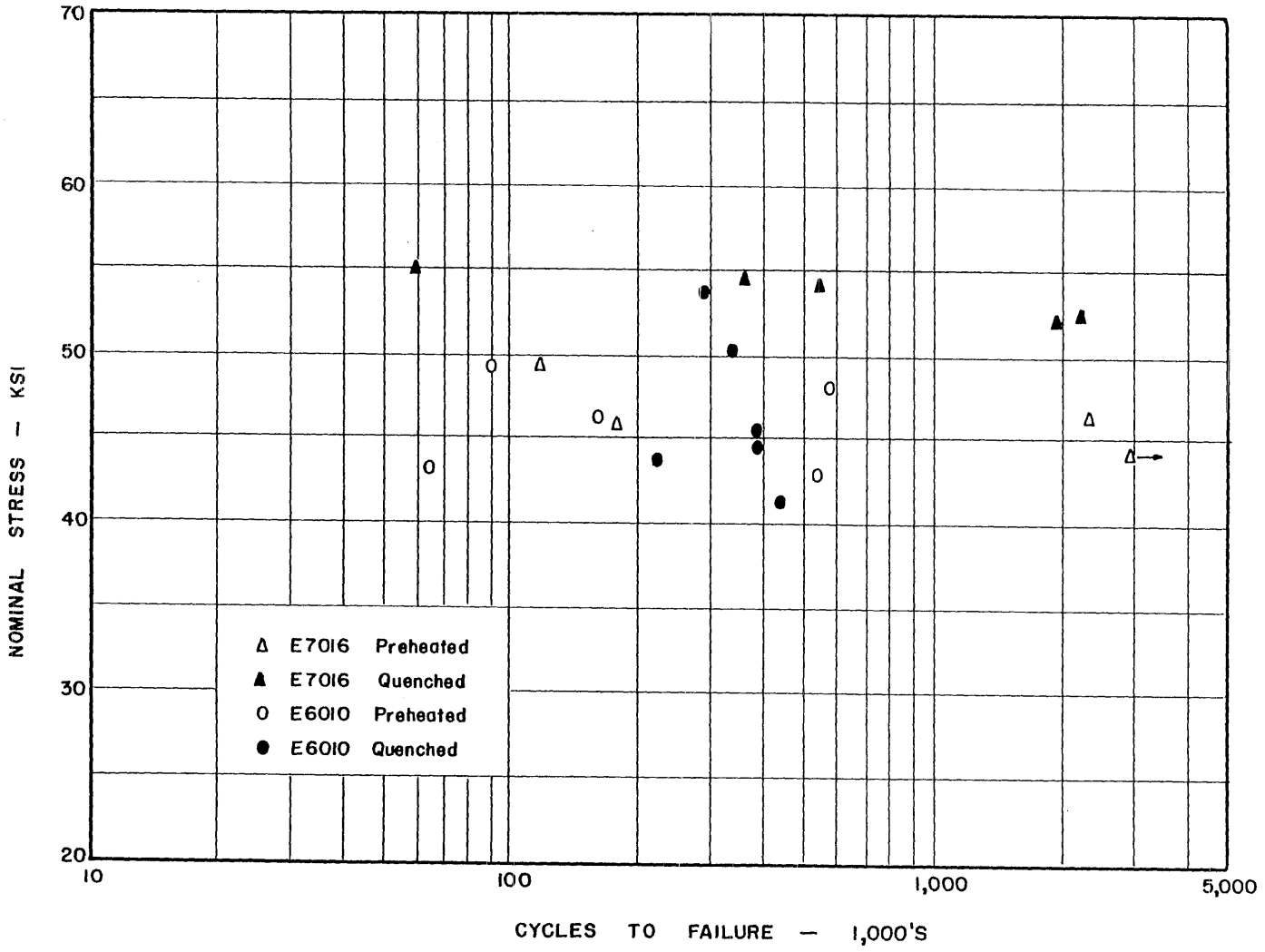

FIG. 16 RESULTS OF FATIGUE TESTS OF TRANSVERSE TYPE C SPECIMENS IN TERMS OF NOMINAL STRESS

00C31

00C74

a. PREHEATED E6010

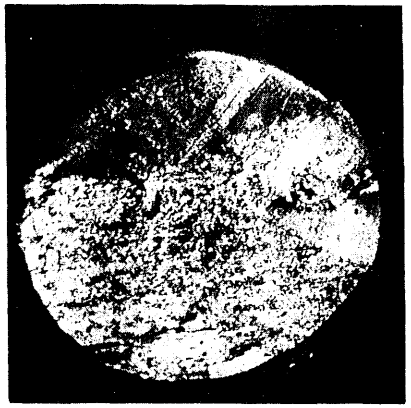

60C37

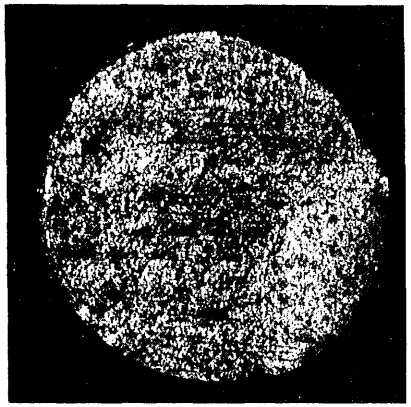

60C71

b. PREHEATED E7016

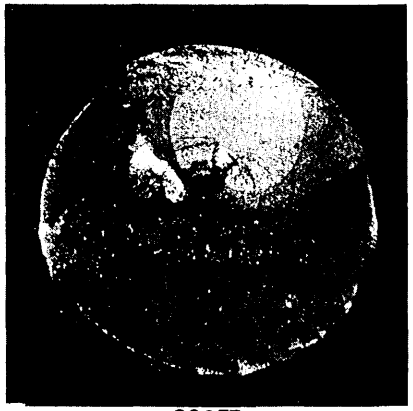

02C57

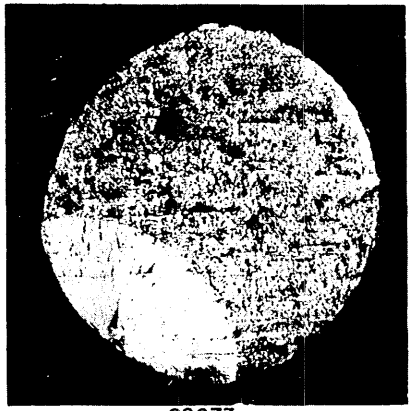

02C73

c. QUENCHED E6010

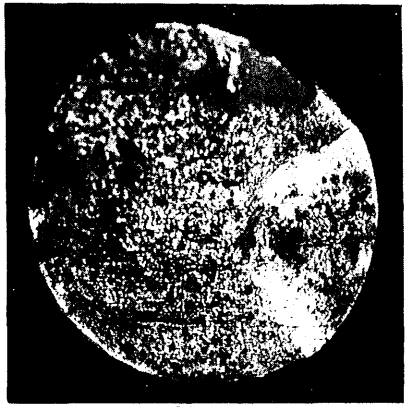

62C62

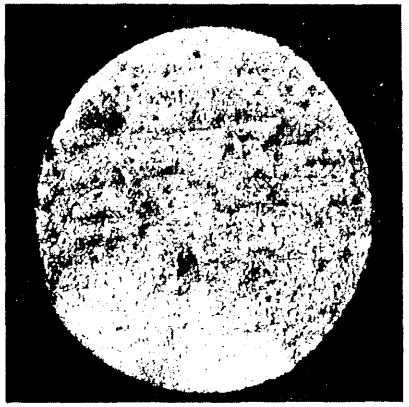

62C68

d. QUENCHED E7016

FIG. 17 PHOTOGRAPHS OF FRACTURE SURFACES OF TRANSVERSE TYPE C FATIGUE SPECIMENS

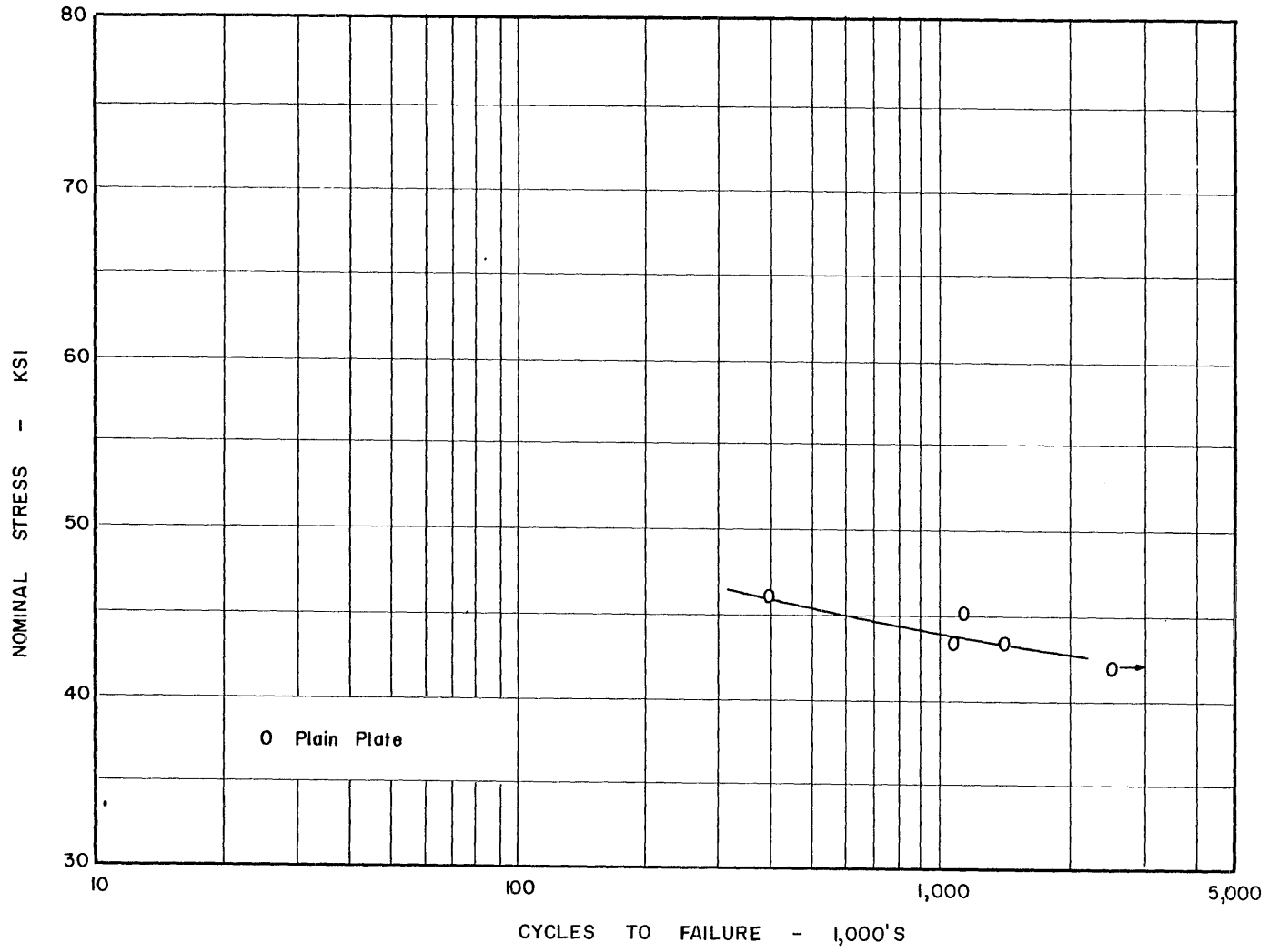

FIG. 18 RESULTS OF FATIGUE TESTS OF TYPE D PLAIN PLATE SPECIMENS IN TERMS OF NOMINAL STRESS

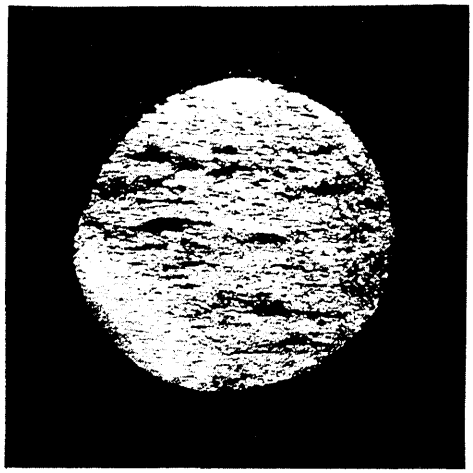

BXB1

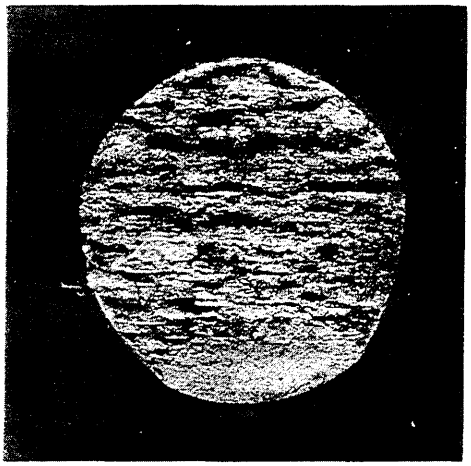

BXB5

FIG. 19 PHOTOGRAPHS OF FRACTURE SURFACES OF PLAIN PLATE TYPE D FATIGUE SPECIMENS

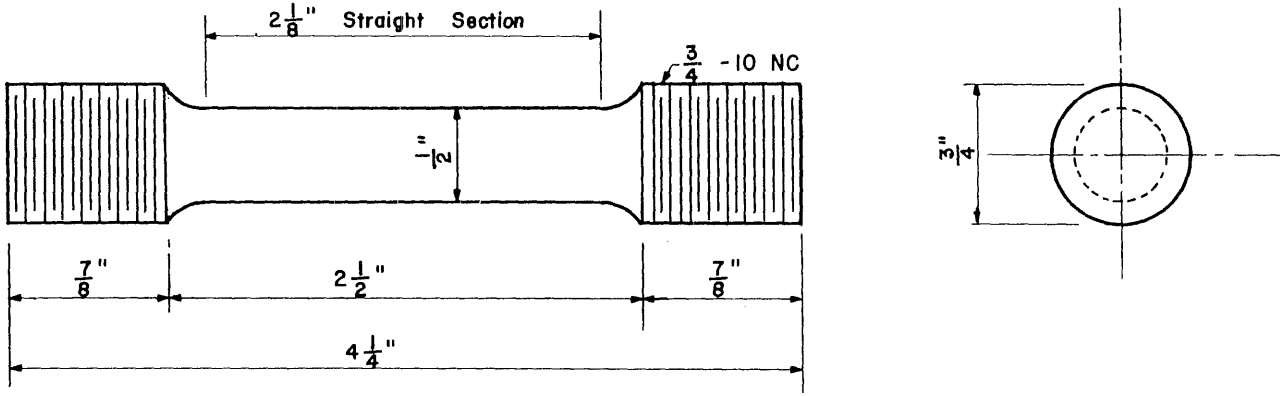

FIG. 20 DETAILS OF TENSILE SPECIMENS

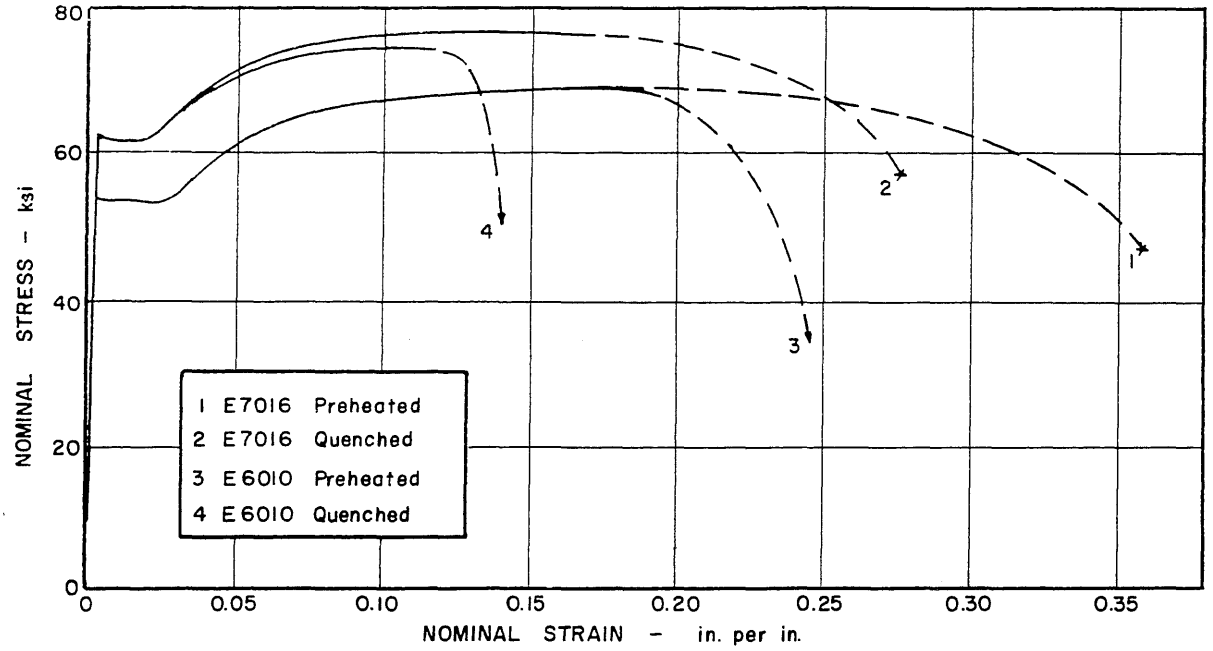

a. NOMINAL STRESS-STRAIN DIAGRAM

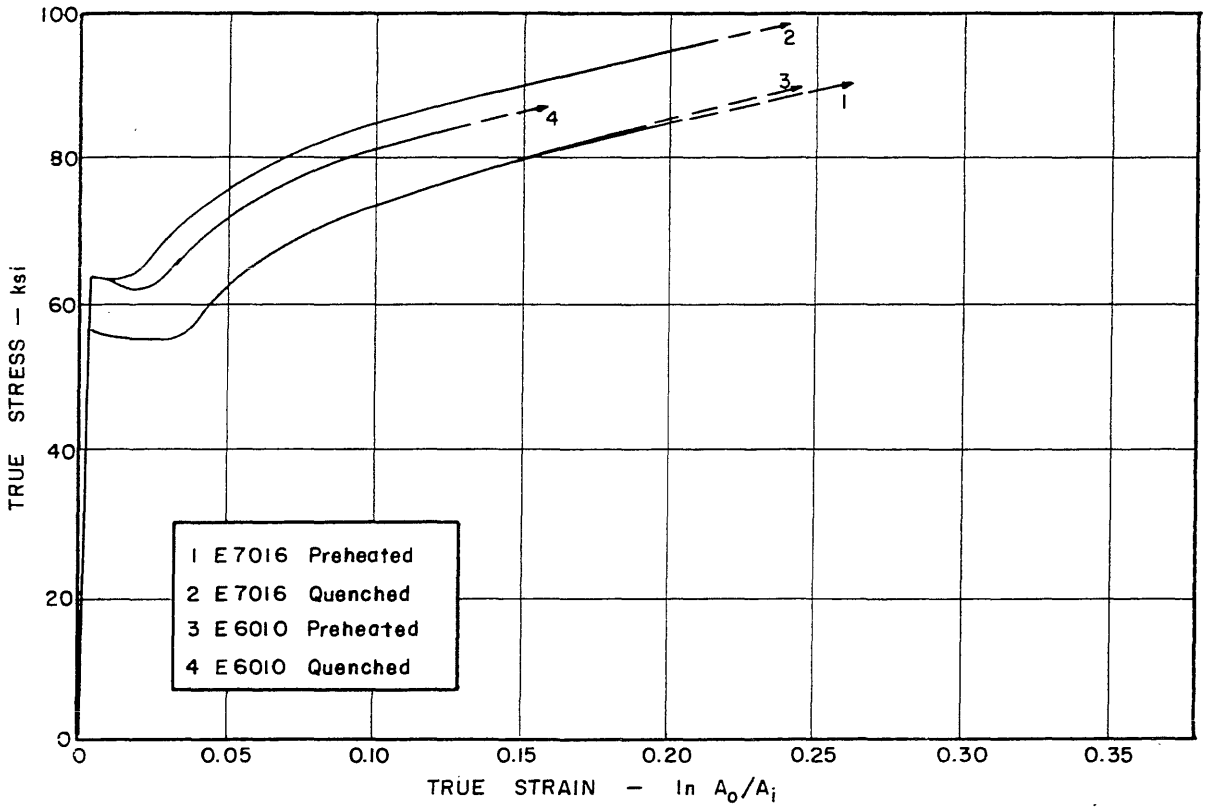

b. TRUE STRESS - TRUE STRAIN DIAGRAM

FIG. 21 STRESS-STRAIN DIAGRAMS FOR STATIC TENSILE TESTS OF LONGITUDINAL ALL-WELD-METAL SPECIMENS - TYPE AT

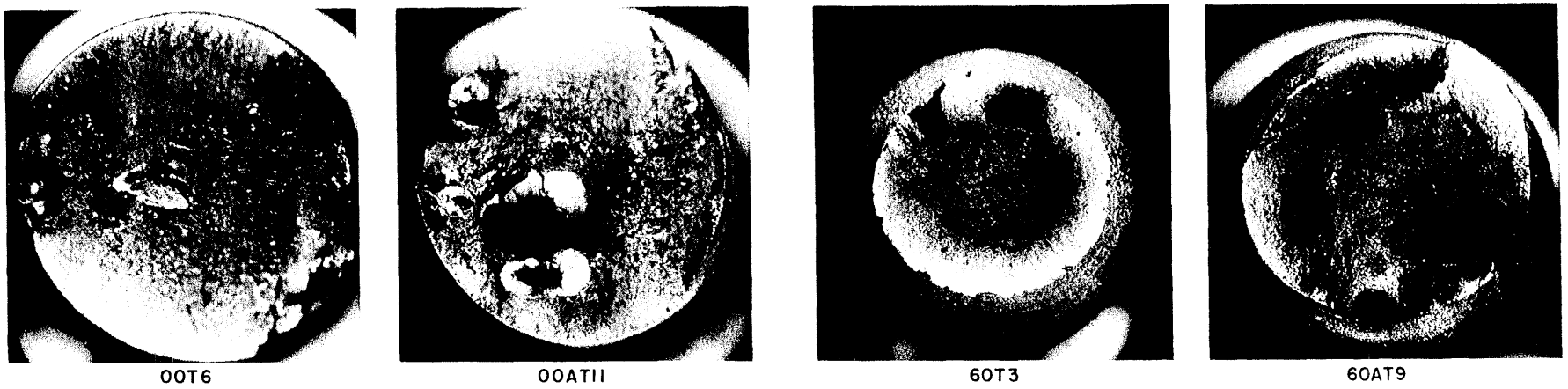

a. PREHEATED E6010

b. PREHEATED E7016

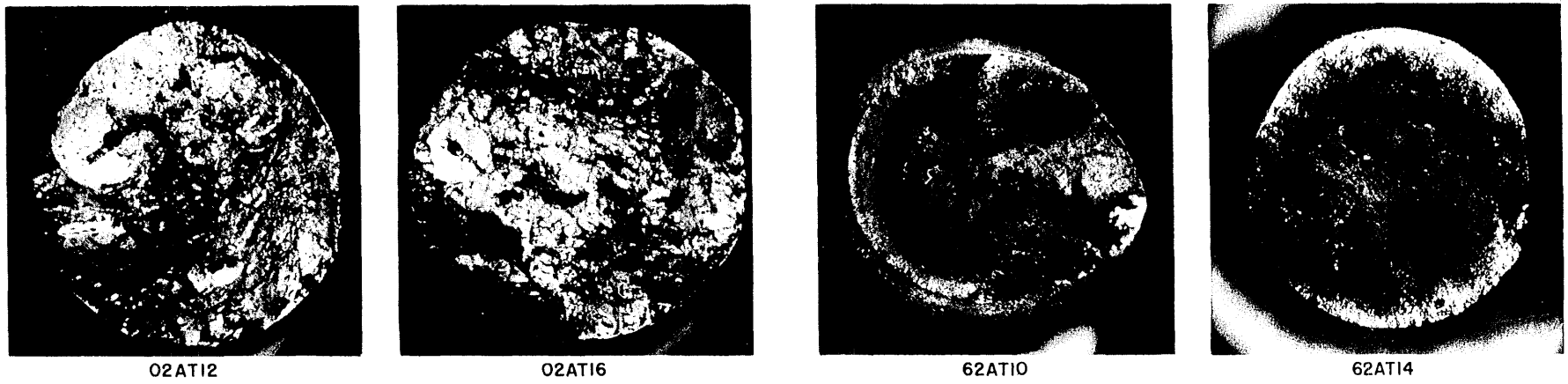

c. QUENCHED E6010

d. QUENCHED E7016

FIG. 22 PHOTOGRAPHS OF FRACTURE SURFACES OF LONGITUDINAL TYPE AT TENSILE SPECIMENS

00BT17
PREHEATED E6010

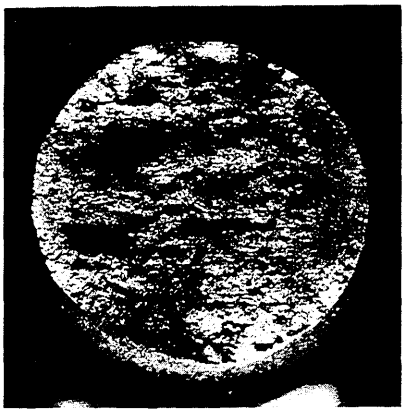

60BT23
PREHEATED E7016

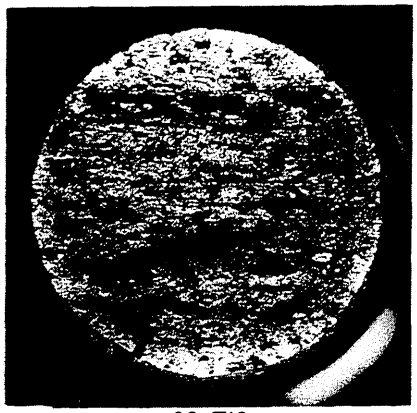

02BT18
QUENCHED E6010

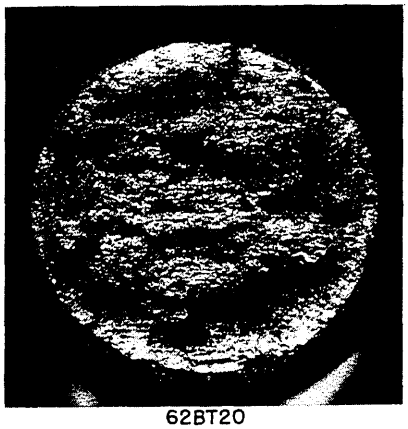

62BT20
QUENCHED E7016

a. TRANSVERSE TYPE BT WELD SPECIMENS

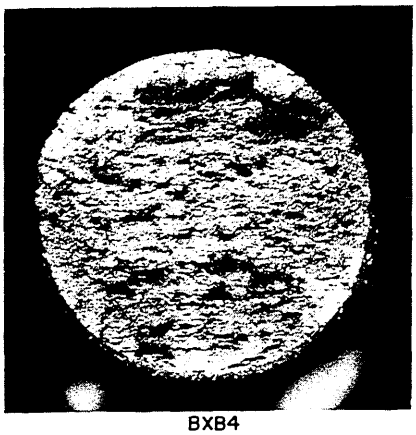

BXB4

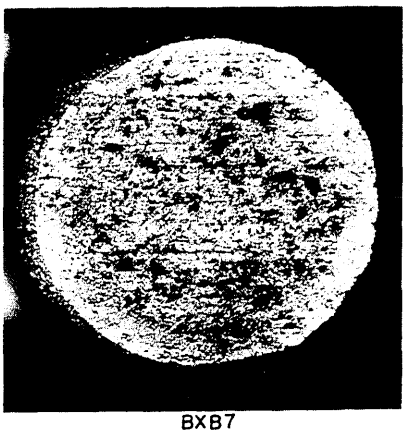

BXB7

b. TRANSVERSE TYPE DT PLAIN PLATE SPECIMENS

FIG. 23 PHOTOGRAPHS OF FRACTURE SURFACES OF TRANSVERSE TYPES BT AND DT TENSILE SPECIMENS

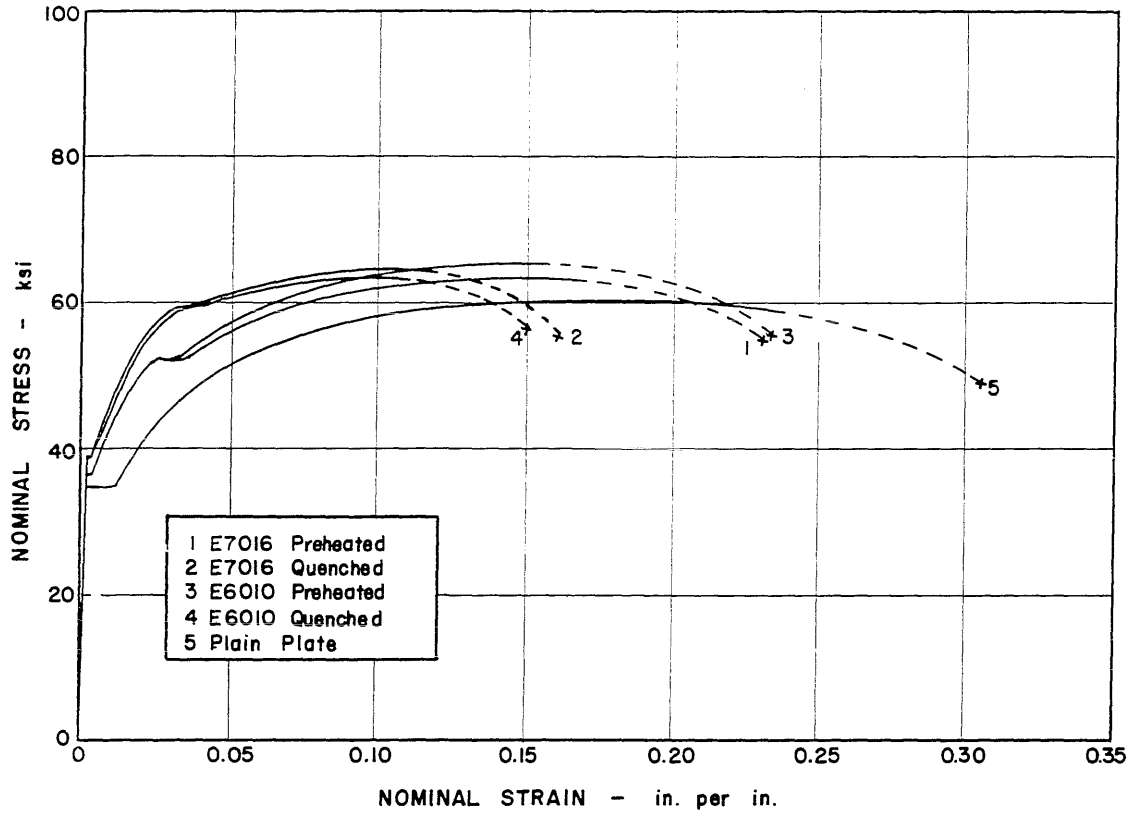

FIG. 24 STRESS-STRAIN DIAGRAMS FOR STATIC TENSILE TESTS OF TRANSVERSE WELD SPECIMENS - TYPE BT, AND PLAIN PLATE SPECIMENS - TYPE DT